TNO PUBLIC

Energy Transition
Princetonlaan 6
3584 CB Utrecht
P.O. Box 80015 3508
TA Utrecht The
Netherlands

www.tno.nl

T +31 88 866 42 56
F +31 88 866 44 75

TNO report - TNO 2022 R12275

Literature review on natural seepage and human-induced leakage of methane at the North Sea and the Gulf of Mexico

Date	6 January 2023
Author(s)	Jasper Griffioen Kees Geel
Reviewers	Jurgen Foeken, Gulnazira Kunakbayeva

Copy no	
No. of copies	
Number of pages	51 (incl. appendices)
Number of appendices	0
Sponsor	International Association of Oil and Gas Producers (IOGP)
Project name	Methane seepage literature review
Project number	060.52953

Preface

Methane is a strong greenhouse gas and its emissions are of wide concern, especially in relation to climate change. The International Association of Oil and Gas Producers (IOGP) asked TNO to prepare a literature overview on the natural and man-induced methane emissions for the North Sea and the Gulf of Mexico. This study aims to present a structured overview of scientific, publicly available data on the natural and man-induced methane emissions for the North Sea and the Gulf of Mexico as related to release from the seabed. Chapter 1 presents the Introduction in which the framework of the project is explained, and Chapter 2 presents the methods employed. Chapter 3 provides background information on global methane emissions and a brief introduction to the biogeochemistry of marine methane. Chapters 4 and 5 present the findings for the North Sea and the Gulf of Mexico, respectively. In these chapters, the geology of the two oil and gas provinces is first explained along main lines. Subsequently, the natural seepage becomes addressed and, finally, the human-induced leakage. Atmospheric emissions also become addressed for both study areas and both sources. Site-specific data on methane fluxes is compiled as much as possible for both situations. Chapter 6 intercompares the findings and evaluates the data availability. Finally, Chapter 7 provides a concluding summary.

Contents

1 Introduction

In marine environments both natural and man-induced emissions occur of the greenhouse gas methane. Many natural seeps and vents are found at the bottom of seas and oceans and part of the methane (or natural gas) released may reach the atmosphere by rising through the water column and degassing at the sea-air interface (henceforth referred to as ''natural seepage''). Another part gets transformed or immobilized by physical and biogeochemical processes. A third part gets dissolved in sea water and may be released at a later stage to the air or stays dissolved contributing to the increasing concentration of methane in seawater. Man-induced leakage of methane (or natural gas) from the seabed also occurs due to gas flow from subsurface methane-bearing layers along or through offshore oil and gas wells (henceforth referred to as ''man-induced leakage''). Comparable attenuating processes are operational for such emissions before released methane escapes to the air. Other man-induced emissions of methane are also present in the marine environment such as leakage from horizontal seabed gas pipelines but such emissions lie outside the scope of the present study.

Insight in both types of emissions from the seabed is of general interest in order to estimate their contributions to the global methane budget. Methane seepage or leakage has been shown to occur as a natural venting process where it is associated with tides, with the presence of salt diapirs, and with faults. Some recent publications have attributed methane leakage in the vicinity of wells to the process of drilling these wells (Vielstädte et al., 2017; Böttner et al., 2020), but this has been questioned amongst others by TNO (Wilpshaar et al., 2021). Unfortunately, natural seepage and man-induced leakage have not been systematically monitored. However, a number of case studies are well documented, especially for the North Sea area and (the American part of) the Gulf of Mexico.

The International Association of Oil and Gas Producers (IOGP) asked TNO to prepare a literature overview on the natural and man-induced methane emissions for the North Sea and the Gulf of Mexico. The aim of this desk study is to provide a structured overview of scientific and publicly available data on this topic for the two regions. The results should provide insight into the size of natural seepage versus human-induced leakage of methane. TNO conducted the work independently and used publicly available sources of information in particular peer- reviewed publications. The activities consisted of: 1. collection of literature, 2. structuring of data and information and 3. categorising reviewed data.

This report contains four more chapters. Chapter 2 presents the methods employed. Chapter 3 contains a brief overview of global methane emissions and biogeochemistry of marine methane. Chapters 4 and 5 present data on methane fluxes, concentrations and geological background information for the North Sea and the Gulf of Mexico, respectively.

2 Methods

This report presents a literature study. TNO built upon earlier literature reviews for the North Sea (TNO, 2018; Wilpshaar et al., 2021). The literature review for the Gulf of Mexico was novel for TNO. TNO used scientific search machines such as Google Scholar and Scopus as well as the regular search machines at the internet. In this way, TNO obtained peer-reviewed literature together with grey literature that is publicly available and web pages. Used keywords were: methane, North Sea, Gulf of Mexico, seep, leakage, well, gas, remote sensing, satellite, Deepwater Horizon.

Secondly, limited attention was paid to remote sensing studies on methane fluxes as they cannot always distinguish between the various sources: methane originating from natural seepage, originating from within the water column, from leakage along/through oil and gas wells, and from platforms, gas pipelines and other infrastructure present (cf. Yacovitch et al., 2020; Irakulis-Loitxate et al., 2022).

Attempts were made to categorise the literature on methane fluxes into three major sources of methane:

1. Natural seepage to the seabed
2. Leakage from commercially exploited reservoirs
3. Leakage from other methane-bearing layers via wells (often called ''shallow gas'' within the context of the North Sea).

Distinction between the last two sources was more feasible for the North Sea than for the Gulf of Mexico. By “Shallow Gas” we mean gas occurrences at subsurface depths shallower than 1000 m (Verweij et al, 2018).

Further, data on fluxes and aqueous concentrations of methane were categorised into the following interfaces and compartments:

- fluxes from the seabed
- concentrations within the water column
- fluxes between surface water bodies (only for the North Sea region)
- fluxes (also called emissions) at the sea-air interface

Frequently, gas fluxes are presented in gas volume per unit time where the pressure is not equal to atmospheric. The gas law was used to convert this to a weight basis:

$$P.V = Z.n.R.T$$

Where P is pressure, V is volume, Z is compressibility factor that accounts for non-ideal behaviour at large depth, R is the gas constant and T is absolute temperature. Z was set to 0.76 instead of 1.0 (Weber et al., 2014) when the depth was large (e.g. 1300 m). In our calculations to covert gas volume to mass of gas, pressure was sometimes estimated as the depth (in m) divided by 10.

3 Global methane budgets and biogeochemistry of marine methane

3.1 Global budgets

A brief overview of global methane budgets is presented below that is mainly based on Saunois et al. (2020). We realise that other numbers may be around in other literature, but it was beyond the scope of this study to (critically) assess the global budgets on methane and the literature behind it. Moreover, the paper by Saunois et al (2020) is arguably decisive, as it has been written by 91 authors from dozens of research institutes that collect data and model emissions, both bottom-up and top-down.

The focus in global methane budget studies is on atmospheric emissions as methane is the second most important human-influenced greenhouse gas with respect to climate forcing. For the 2008–2017-decade, global methane emissions are calculated to be 550-594 Tg y^{-1} based on atmospheric inversions (note 1 Tg = 1 megatonne = 1 Mtonne), which is called the top-down approach. According to bottom-up methods in which the individual sources get summed, the global emissions are 594-881 Tg y^{-1}. There is a considerable gap between these two ranges. and it has been assumed that the emissions of some of the sources are overestimated (Saunois et al., 2020).
With respect to the sources, distinction is made between natural and anthropogenic origins. The processes in which emitted methane was produced may be biogenic, thermogenic or pyrogenic. Biogenic methane is produced from decomposition of organic matter by Archaea in anaerobic environments. Thermogenic methane refers to breakdown of buried organic matter under elevated temperature and pressure. Pyrogenic methane is from incomplete combustion of biomass and other organic material. Peat fires and biofuel burning are examples of the latter.

Table 1: Averages and ranges in atmospheric methane emissions from various anthropogenic sources for the period 2008- 2017 (Saunois et al., 2020).

Source	Annual emission (Tg methane y^{-1})
Agriculture and waste	
1. Livestock (domestic ruminants and manure)	111 [106-116]
2. Landfills & waste	65 [60-69]
3. Rice cultivation	30 [25-38]
Fossil fuels	
4. Coal mining	42 [29-61]
5. Oil & gas	80 [68-92]
6. Industry	3 [0-7]
7. Transport	4 [1-12]
Biomass & biofuel burning	
8. Biomass burning	17 [14-26]
9. Biofuel burning	12 [10-14]
Total	366 [349-393]

Table 1 presents averages and ranges ranges in anthropogenic methane emissions that were established using bottom-up approaches. The corresponding range from the top-down approach is 336-376 Tg y^{-1} for the total anthropogenic emission, which shows considerable overlap. According to the table, the largest source is livestock, followed by landfills & waste and oil & gas. The oil & gas subcategory includes emissions from both conventional and shale oil and gas exploitation. Both fugitive and planned emissions during the drilling of wells in gas fields, extraction, transportation, storage, gas distribution, end use, and incomplete combustion of gas flares emit methane and are included in this subcategory (Saunois et al, 2020)

The ranges for the natural sources are presented in Table 2. The corresponding range from the top-down approach is 183-248 Tg y^{-1} for the total global emission. Here, the range for Wetlands has considerable overlap with 159-200 Tg y^{-1} whereas that for other natural sources is only 21- 50 Tg y^{-1}. A large discrepancy thus exists. Wetlands are recognised as a major, natural source of methane. Surface water bodies are supposed to be the largest source under other land sources followed by Geological sources. Five categories were distinguished under Geological sources:

1. On-land gas–oil seeps,
2. Mud volcanoes,
3. Diffuse micro seepage, and
4. Geothermal manifestations including volcanoes.
5. Submarine seepage

On-shore micro seepage is considered to be largest source with 24 Tg. The other values are 4.7 Tg yr^{-1} for geothermal manifestations, about 7 Tg yr^{-1} for submarine seepage, and 9.6 Tg yr^{-1} for onshore seeps and mud volcanoes. These numbers are partly derived from Etiope & Schwietzke (2019). An inverse calculation based on $^{14}CH_4$ trapped in ice cores suggests 0.1 - 5.4 Tg y^{-1} (95%) for global geological emissions (Hmiel et al., 2020). This result was strongly critised by Thornton et al. (2021). Weber et al. (2019) also obtained values for the total oceanic emission that are in the lower end of the range. These estimations were based on machine learning calculations using aqueous methane concentrations combined with constraints on bubble-driven ebullitive fluxes resulting in a figure of 6-12 Tg y^{-1} and where shallow near-shore environments were believed to produce the largest contribution.

In Table 2, the range for marine seepage refers to the emission at the sea-air interface. US- EPA (2015) estimated marine seepage from the seabed as 8-65 Tg y^{-1}. The difference is explained by physical and biogeochemical processes at the seabed and in the water column, as discussed in the next chapters for the North Sea and the Gulf of Mexico.

Table 2: Ranges in atmospheric methane emissions from various natural sources for either 2008-2017 (Wetlands) or 2000-2009 (others; Saunois et al., 2020).

Source	Annual emission (Tg methane y^{-1})
Land sources	
1. Wetlands	102-182
2. Surface water bodies	117-212
3. Geological	13-53
4. Wild animals	1-3
5. Termites	3-15
6. Permafrost soils	0-1
7. Vegetation	Uncertain and partly included under wetlands
Oceanic sources	
8. Geological	5-12
9. Biogenic	4-10
Total	245-488

3.2 Biogeochemistry of marine methane

Methane that originates from the subsurface either naturally or from man-induced actions may undergo various processes that cause atmospheric emissions to be substantially lower than associated fluxes at the seabed. The following processes are relevant:

- Anaerobic methane oxidation in the shallow seafloor sediments with associated uptake in carbonates (Methane Derived Authigenic Carbonates, or MDAC).
- Formation of gas hydrate from methane-supersaturated fluids at sufficient depth (> 60 bar, equivalent to 600 m) and low temperature (< 4°C; Suess, 2010). A gas hydrate is like ice, where the low molecular weight gas molecule is surrounded by a cage of frozen water molecules.
- Dissolution of gas bubbles while rising through the water column with associated expansion of bubbles at decreasing depth and partitioning of dissolved air into the bubbles.
- Dispersive mixing of methane-rich seawater with surrounding methane-poor seawater.
- Entrapment of methane at the marine pycnocline/thermocline.
- Aerobic oxidation of methane in the water column.

The fraction of seeped methane that reaches the sea-air interface therefore is strongly dependent on various factors such as: water depth, size of initial bubbles, whether oil is associated with bubbles etc.

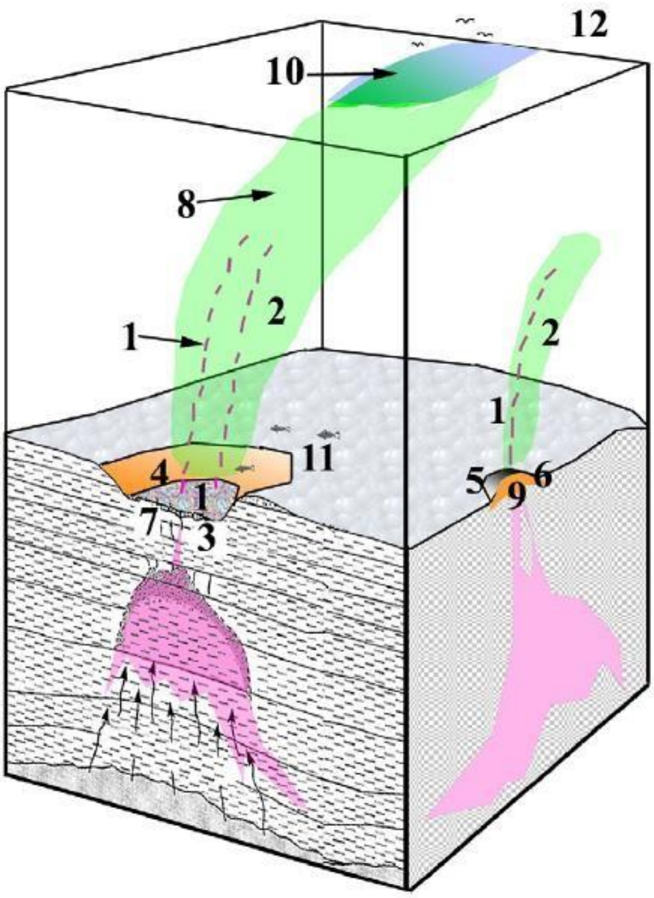

Figure 1: Drawing showing some of the characteristic features of macroseeps with 1. Ebullition of bubbles, 2. Hydroacoustic flares, 3. Methane concentration anomalies, 4. Aureoles, 5. Topographic expressions, 6. MDAC development, 7. Bacterial mats, 8, upwelling seawater, 9 downwelling water or entrainment, 10 slicks and nutrients at the seawater surface, 11 enhanced biodiversity, 12 methane anomalies in the air (d*erived from Hovland et al., 2012). Note that the role of gas hydrates is not indicated in this drawing. This is a specific feature for the deeper parts of the Gulf of Mexico but not for the North Sea (https://www.usgs.gov/media/images/map-gas-hydrates).*

It should be noted that field observations indicate that gas fluxes at the seabed vary in time over periods of weeks/months (e.g., Hu et al., 2012; Jerram et al., 2015; Meurer et al., 2021). Many numbers presented are based on a single investigation but may thus differ over time. For example, the figure below shows how seep intensity may vary over time for Bush Hill site, a major seep in the Gulf of Mexico, due to precipitation of gas hydrate. Small shallow gas reservoirs are formed under impermeable gas hydrates that get formed. When gas bursts to surface seepage intensity at seabed is elevated until the reservoir deflates and the driving force of seepage dissipates. The appearance and disappearance of shallow gas reservoirs and subsurface bubbles also induces pore water flow into the seabed or not to compensate outflowing volumes of gas and water.

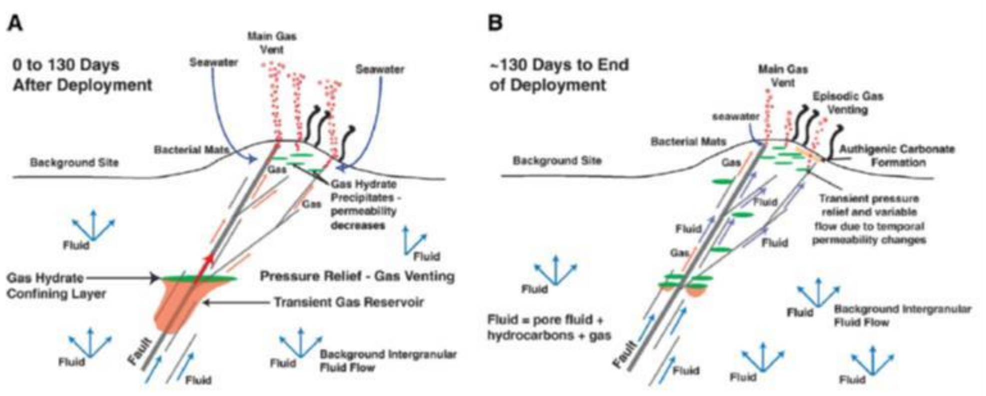

Figure 2: Conceptual model of the Bush Hill site. Distance covered is 50 m horizontally and 100 m vertically. Left figure depicts stage in which a confining layer traps migrating gas leading to overpressurization and fracturing. Right figure depicts background fluid flow field derived from Solomon et al. 2008). Deployment refers to the deployment of remote operated vehicles and does not refer to the feature itself.

Microbial oxidation of methane in the water column has frequently been demonstrated. There is a threshold concentration of 3-10 ng CH_4 L^{-1}, above which oxidation can be substantial and below which it is very slow (Valentine et al., 2001; Damm et al., 2005). First-order oxidation rates of 0.0004 – 0.05 day^{-1} have been established for marine, arctic to tropical conditions (De Angelis, 1993 and cited references). This implies half-life times of 14 days to 5 years.

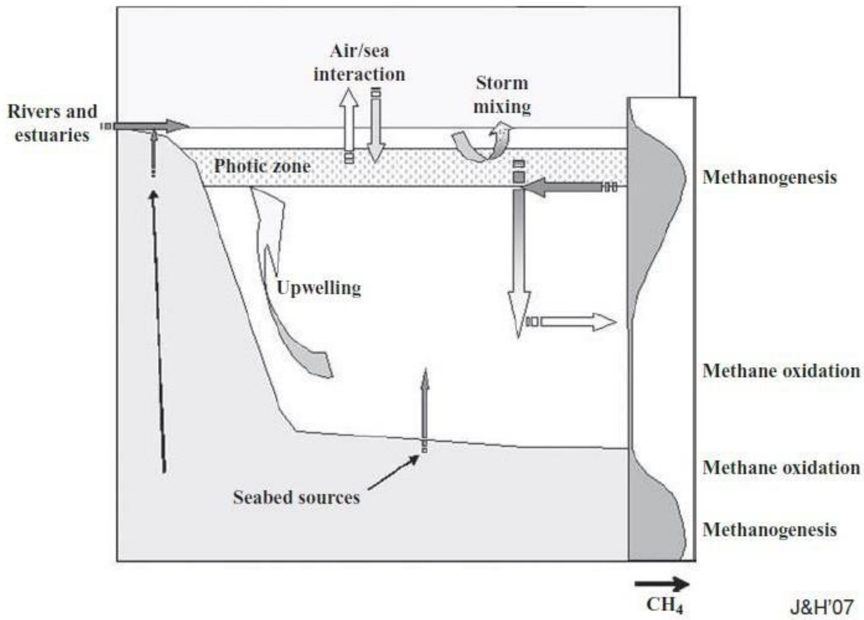

Figure 3: Methane cycling on oceans with methane release from the seabed (from seeps or not) and methane production in the photic zone (derived from Judd & Hovland, 2007).

Biogenic methane may also be produced at seeps due to anaerobic degradation of organic matter. Seeps are usually fertile environments so biological productivity is high and anaerobic environments may establish from which methanogenesis occurs. This is especially documented for the Gulf of Mexico region (e.g., Fisher, 2007). Methane may also be produced in the water column by degradation of dissolved organic matter phosphonates or marine algae (Bizic et al., 2020). The methane concentration may then lie above the value for equilibrium with air, which is 2 nmol CH_4 L^{-1}. This may cause elevated concentrations directly above the seabed and in the shallow, photic zone with low concentrations in between (*Figure 3*).

4 North Sea

4.1 Introduction

The North Sea contains major gas reservoirs and shallow gas is also frequently found. Oil and gas are produced at the North Sea and the existence of natural seepage is also well known. The natural seeps have been studied at the North Sea as has human-induced leakage of methane or natural gas.

The North Sea is a shallow sea in Northwest Europe bordered by the UK, Norway, Denmark, Germany, The Netherlands, Belgium, and France. It measures some 1000 by 600 km and connects to the Atlantic Ocean through the English Channel in the south and the Norwegian Sea in the north. Its northern boundary with the Norwegian Sea is a bit arbitrary but is taken here as the line Orkney Islands-Shetland Islands-Ålesund. Water depths range from a few tens of meters in the south to several hundred meters in the North, off the coast of Norway (*Figure 4*).

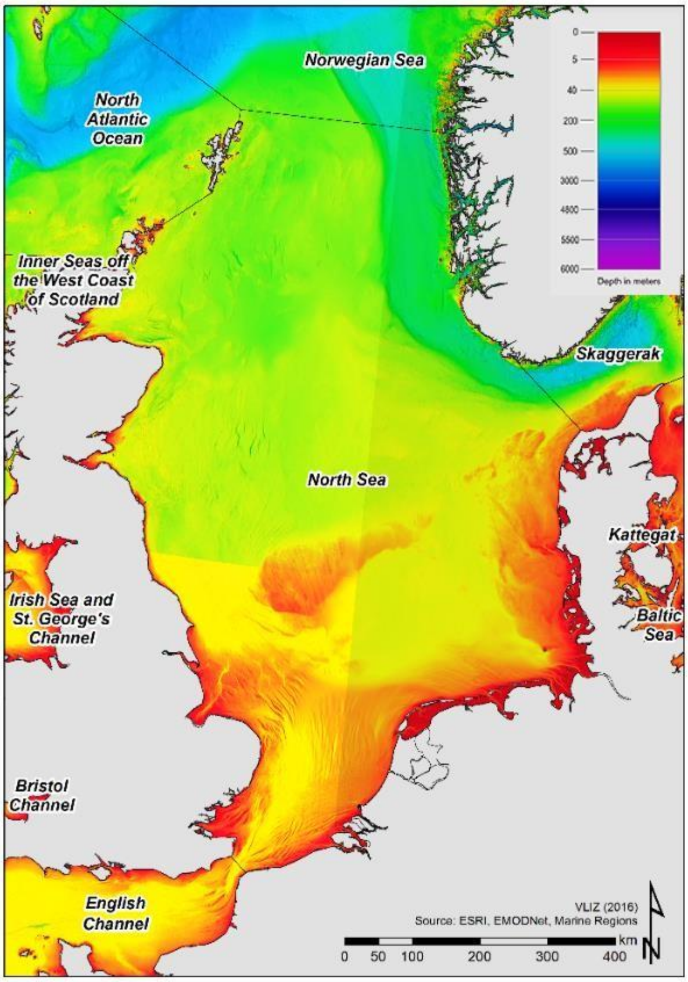

Figure 4: Bathymetry of the North Sea (Marinesources.org).

4.2 Geology

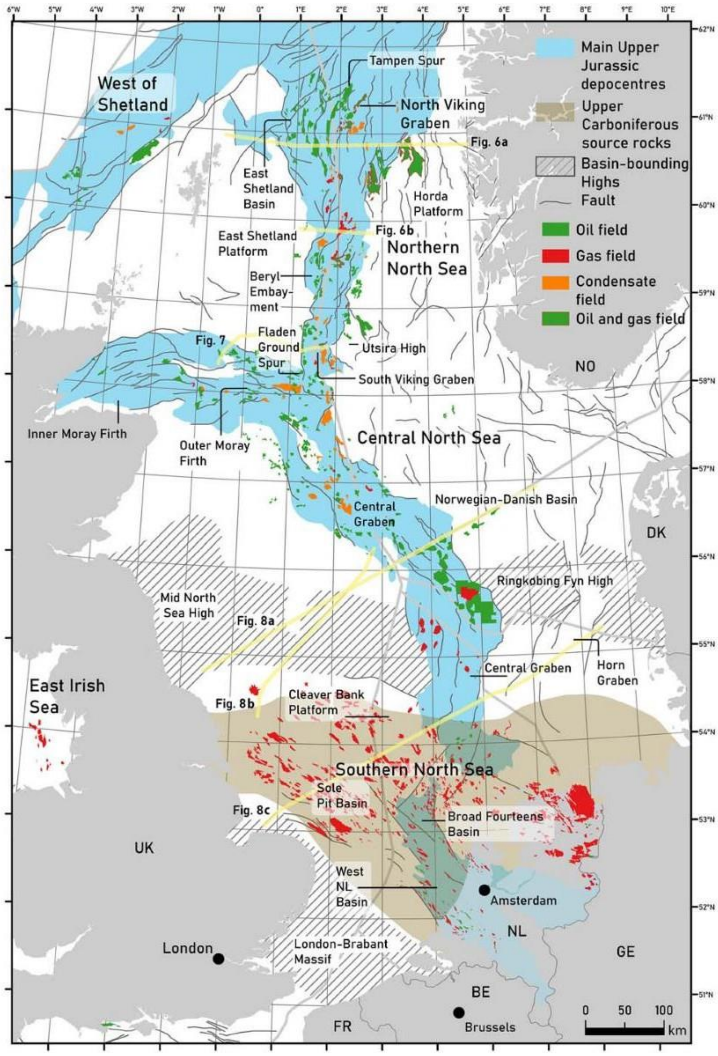

Figure 5: Location map of the North Sea Basin, showing the main Late Jurassic and Late Carboniferous depocentres that host the two main source rocks, oil and gas discoveries to date and the seismic line locations shown in Figure 9 to Figure 11. After Patruno et al (2021).

4.2.1 Oil and gas exploration

Exploration for oil and gas in the North Sea started shortly after the discovery of the giant Groningen Gas Field onshore The Netherlands in 1959. The First Round of UK Licensing was in 1964, after which the first offshore hydrocarbon fields were discovered in 1965. Initially, exploration efforts were directed towards finding analogues of the Groningen Field which resulted in the 'Southern Gas Boom' (Bowen, 1991). Since the early 1970's, starting with the discovery of the Forties and Brent fields, exploration focus was more on oil in the central and northern North Sea. This resulted in the discovery of large volumes of oil in multiple fields in Jurassic and Tertiary Sandstones, draped over structural horsts or in tilted fault blocks in the grabens.

Oil and gas fields are not evenly distributed across the North Sea (*Figure 5*). Most of the oil and condensate fields are found in or near one of the grabens that form the Mesozoic rift system: the Central Graben, the Moray Firth, and the Viking Graben. Most of the gas fields, on the other hand, are located in mainly Permian sands in the Southern North Sea, in a E-W trending belt from Northern Germany, via The Netherlands, to the UK continental shelf (UKCS).

As a petroleum basin, the North Sea is mature, as testified by several creaming curves (*Figure 6*, *Figure 7*). Also, the number of wells drilled to date is large: in 2013, more than 23,000 wells have been drilled (Vielstädte et al, 2017); even when sidetracks and multilaterals are excluded the number is still 15,781. Oil and gas production has been gradually decreasing after having reached its peak in the UK in the mid-nineties (*Figure 8*), and in Norway a few years later (*Figure 8*).

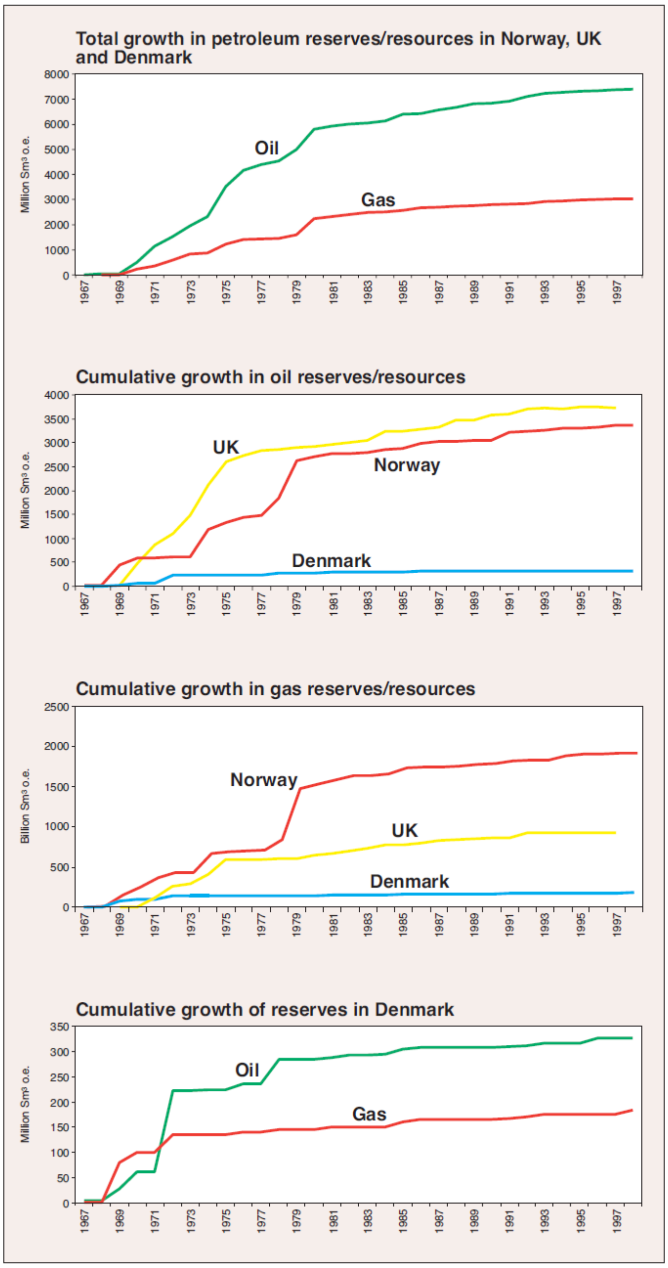

Figure 6: Creaming curves for oil and gas in the North Sea (excluding the southern gas province) for Norway, UK, and Denmark. From Eriksen et al (2003).

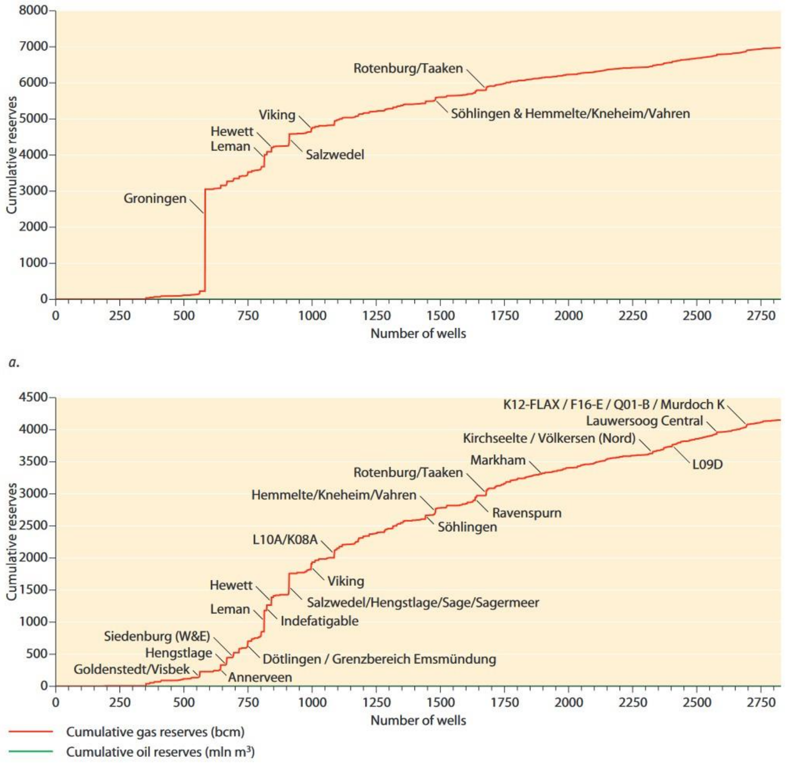

Figure 7: a. Creaming curve for the Anglo-Dutch and North German basins petroleum province; and b. creaming curve for the Anglo-Dutch and North German basins petroleum province, excluding the Groningen field. From Breunese et al (2010).

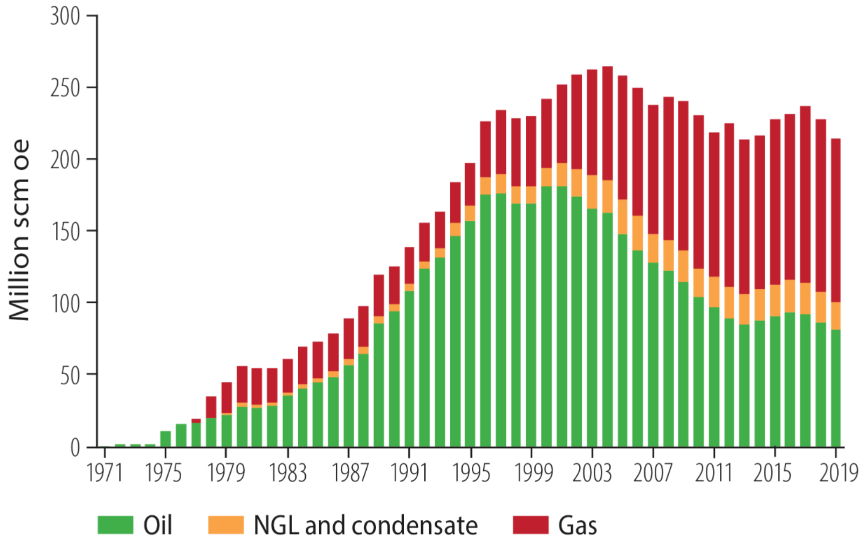

Figure 8: Historical production of liquids and gas from the Norwegian Continental Shelf until 2019 (includes Norwegian Sea and Barents Sea).

4.2.2 Petroleum geology

As mentioned above, the North Sea consists of several different plays. The main gas play is the "Rotliegend fairway" (Van Wijhe et al, 1980), a wide east-west corridor (*Figure 5*) in which all play elements fit together: the reservoirs consist of good-quality aeolian sandstones of Permian Rotliegend age, the source is formed by Carboniferous coal layers, and the seal is provided by thick Zechstein evaporites. Traps are usually tilted fault blocks. The Rotliegend fairway coincides broadly with the southern, sand-prone margin of the Southern Permian Basin (Gast et al, 2010). The thick evaporite series of the Zechstein form an excellent seal. They are in fact so good, that most of the Triassic sandstones in structures above the Rotliegend fairway are dry. This also means that methane leakage from the Rotliegend to the surface is exceedingly limited and will be restricted to those places where the Zechstein seal is either locally missing, or where major faults displace the Zechstein salt to such a degree that a pathway for migration is created.

The majority of the oil that is produced from the North Sea is found in the grabens (*Figure 5*). Sourced mainly by the Jurassic Kimmeridge Clay that is buried deep enough in the grabens to form an active kitchen, the hydrocarbons migrate upward into Jurassic, Cretaceous, and Tertiary sandstones. Seal is usually provided by Cretaceous and Cenozoic mudstones. For the Jurassic reservoirs traps are mostly tilted fault blocks, but the post-rift Upper Cretaceous and Paleocene plays contain traps defined by stratigraphic pinch-outs and drapes over highs (Hill & Woods, 1980).

The tectonic style and history differ from place to place along the rift system, giving rise to different trap configurations and migration pathways. Three examples are discussed below.

4.2.2.1 Northern North Sea

The Viking Graben and its adjacent platforms, the East Shetland Basin to the West and the Horda Platform to the East, host the prolific Brent-type fields (*Figure 9*), both on the UK side and the Norwegian side of the median line. Faults offset the Jurassic and sometimes the Cretaceous, but generally do not extend upward into the Tertiary. A thick Tertiary cover of up to 2 km thick has filled the graben.

4.2.2.2 Central North Sea

The Moray Firth has a slightly different tectonic history than the Central Graben and Viking Graben. Not much of the Jurassic is preserved (*Figure 10*) because of continuous uplift and erosion in the Fladen Ground Spur. As a result, simple, predictable Brent-type fields are not present here. Play types include stratigraphic traps, but also structural traps are quite common. Piercement diapirs in the Central Graben that are linked to extensional faulting over the top of them (Machar, Mungo, Tommeliten etc.) play an important role in seepage in this area. Chalk reservoirs draped over salt pillows are also important in that respect. Reservoirs are of various ages: Paleogene, Chalk, Lower Cretaceous, Triassic, Permian, and even Devonian. Unsurprisingly, there are many different seals in the central part of the North Sea.

4.2.2.3 Southern North Sea

The Southern North Sea area is quite different from the more northerly parts of the Jurassic rift system (*Figure 11*). The main differences are 1) The prolific Kimmeridge Clay is largely absent or has low Total Organic Carbon (TOC); 2) Thick Jurassic sandstones are largely absent; 3) A thick upper Cenozoic deltaic sequence is present.
Therefore, the southern North Sea is basically a gas province, with Carboniferous source rocks, Permian reservoirs, and thick Permian rock salts acting as seal. Shallow, microbial gas is also present in the southern part. In addition, a modest amount of Jurassic oil fields have been found.

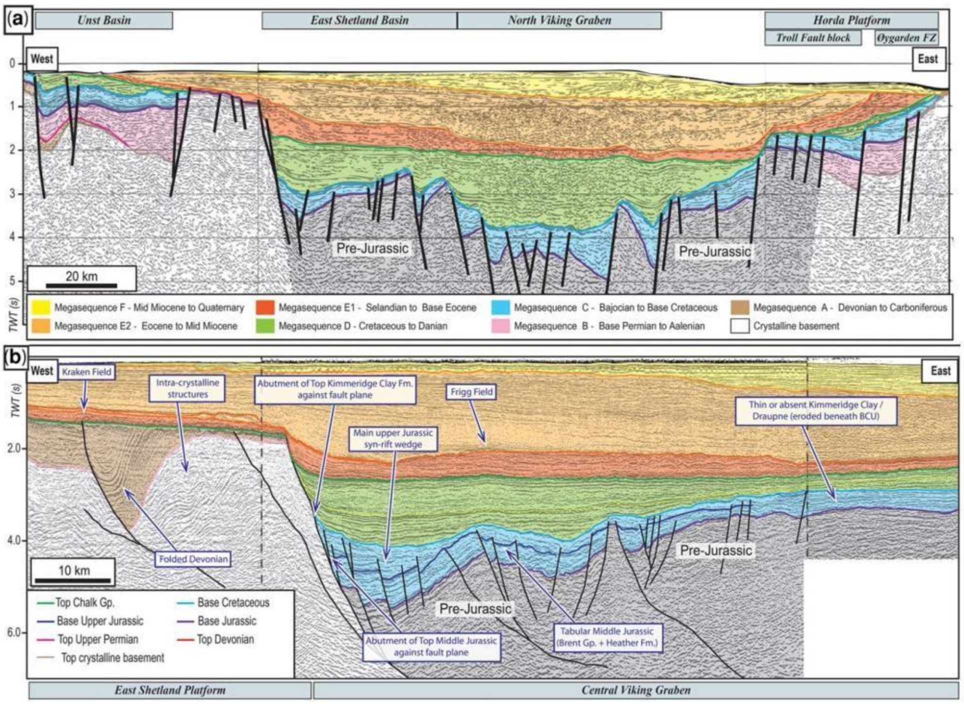

Figure 9: Seismic sections in the Northern North Sea, showing structural style and main depositional units (Patruno et al, 2021).

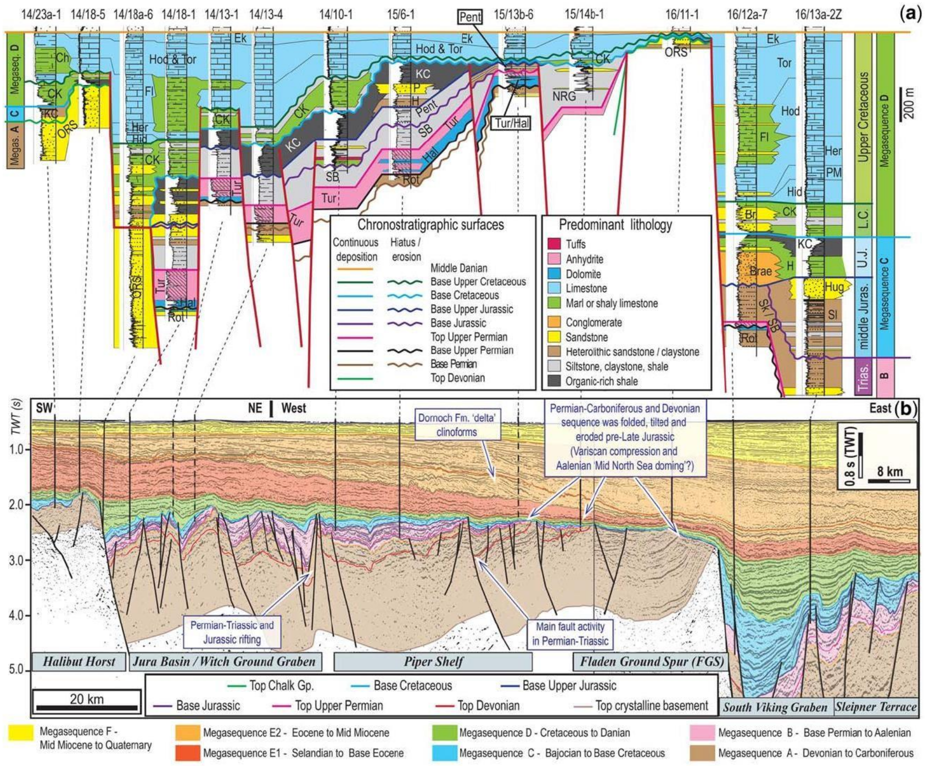

Figure 10: (a) Well panel and (b) seismic section in the Central North Sea. From the Outer Moray Firth to the South Viking Graben area, showing structural style and main depositional units (Patruno et al, 2021).

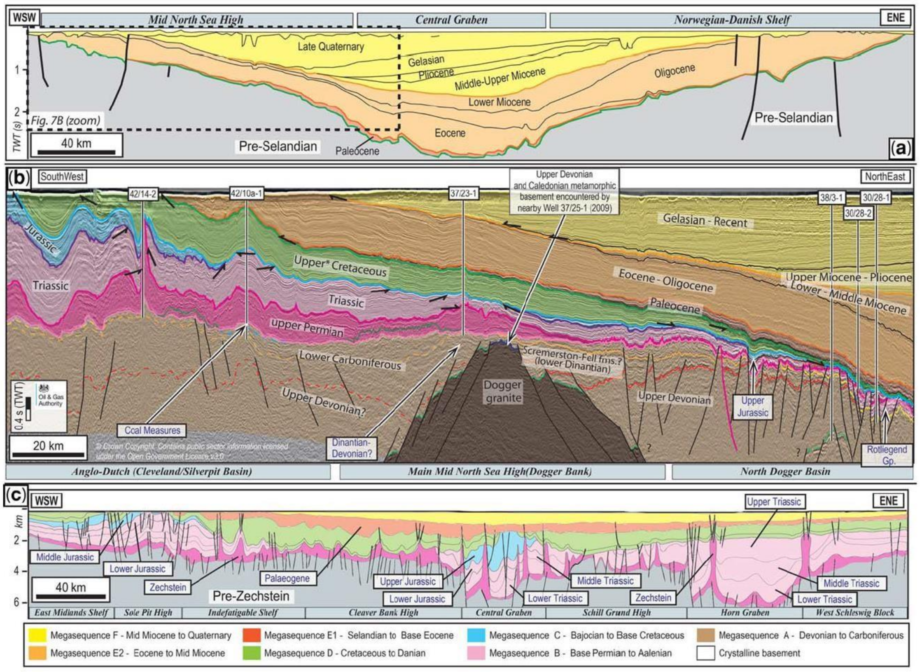

Figure 11: Seismic sections in the Central and Southern North Sea, showing structural style and main depositional units (Patruno et al, 2021).

4.2.3 Source rocks

Most of the oil and gas fields are sourced from either Upper Carboniferous coals or from the Upper Jurassic Kimmeridge Clay (Brown, 1991). A few other source rocks are locally important, such as Devonian lacustrine shales, Lower Carboniferous coals such as the Scremerston Formation and black shales (Bowland Shale) and Lower Jurassic Posidonia shale. In the Southern North Sea, the Pliocene to Quaternary delta deposits contain abundant organic material that has been shown to have sourced the majority of the shallow gas fields in the North Sea through microbial activity (Verweij et al, 2018). The last source rock is of particular importance to shallow gas accumulations and methane seepage in the North Sea.

4.3 Natural seeps

Both natural seepage and human-induced leakage of methane or natural gas have been studied across the North Sea. *Table* 3 presents a compilation of literature data on methane fluxes at individual sites across the North Sea. Both natural seepage and human-induced leakage are addressed where fluxes at the seabed and at the sea-air interface are compiled. When feasible, the fluxes were converted to tonnes of methane y^{-1} which enables easy intercomparison of the figures. For sake of clarity, these fluxes are also depicted in *Figure 13*. *Table 4* presents data on total fluxes for the North Sea or parts of it (including associated estuaries). These values were calculated by combining values for fluxes at individual sites and numbers of sites. Both have their uncertainties which lies beyond the scope of this investigation. The findings for natural seepage and man-induced leakage are discussed below in two separate sections.

The North Sea contains a number of seeps and seep areas. Some of these sites are referred to as macroseeps: Tommeliten, Scanner and Gullfaks (*Figure 12*). Note that no value for the methane flux at Gullfaks is known to the best of our knowledge. The seeps are frequently visually recognised as pockmarks but not all pockmarks are active methane vents. Some of them are relics and must have been active under different conditions. Pockmarks have been found in the northern part of the North Sea and on the British and Dutch continental shelf (Hovland et al., 2012). However, seeps may be present without morphological expressions at the seabed. This may hold when the sediment at the sea bottom is coarse.

When we leave out the value presented by Hovland et al. (2012) for the methane flux as a mistake in copying a value from older reference, we note that the natural methane fluxes at the individual seep areas monitored in the North Sea vary between 4.2 and 1,600-2,700 tonnes y^{-1}. Strikingly, these boundary values refer both to the same Scanner pockmark site. The difference is considerable and may be explained by increasingly better methods to quantify methane fluxes at depth. The ranges reported for both the seep at UK Block 15/25 and Tommeliten lie closer to each other. The German Bight pockmark field (Figure 12; Krämer et al, 2017) emerged recently where a large volume of methane was identified as being emitted in a period of only 3 months.

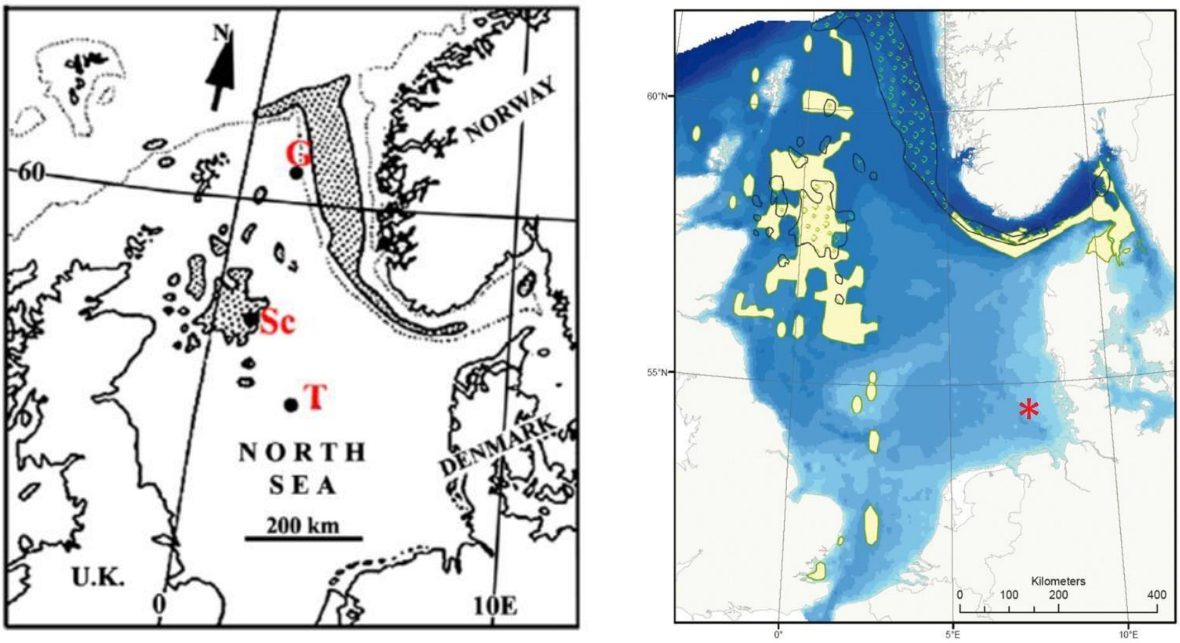

*Figure 12: Locations of macroseeps and pockmark areas in the North Sea.Left: location of 3 macroseeps: G = Gulfax, T =Tommeliten and Sc = Scanner (*derived from Hovland, 2012). *Right: recent indication of pockmark areas in the North Sea (derived from http://www.coastalwiki.org/wiki/ Marine_geo-information_system_for_the_ North_Sea_seafloor). Red star indicates the recent German Bight pockmark field.*

Two studies undertook an upscaling on natural seepage across the UK continental shelf (UKCS) where it holds that most of the seepage is supposed to be present in the North Sea part of the UKCS (Tizzard, 2008; Judd et al., 1997). The two studies present different ranges, and it is not sure whether the more recently established range presents a better estimate. Note that the upper values for the ranges (2,900,000 and 6,200,000 tonnes y^{-1}) lie close to or within the range for oceanic geological seepage which is 5,000,000 – 12,000,000 tonnes y^{-1} (*Table* 3). The fluxes are calculated as a multiplication of seep density and intensity. For the latter, one must realise that Judd et al. (1997) took a global log average as upper limit (35.8 tonnes y^{-1}). Tizzard (2008) used a somewhat larger global dataset and based the lower and upper limit on the 25 and 75 percentiles for seep rate per square meter. An average seep site of 0.14 km^2 was assumed (albeit that the data used on seep size does not show normality but more log normality). The resulting values for flux rate were lowered in order to take into account temporal variation (in a subjective manner as phrased by Tizzard) and gas composition (i.e., no 100% methane). The obtained values for seep intensity are 2.13 and 72.2 tonnes y^{-1}. Both approaches bring forward that the upper value is strongly impacted by taking into global outliers such as Coal Oil Point in front of the Californian coast as well. Alternatively, Vielstädte et al. (2017) came up with a value of 200 tonnes y^{-1} for the total natural seepage from the seabed of the North Sea. This is already lower than has been reported recently for two of the individual seeps or seep areas (Scanner Pockmark and Dutch Dogger Bank). The value was therefore critised by Wilpshaar et al. (2021).

Considerable natural seepage has also been recognised from the methane concentrations measured by Borges et al. (2016) in the Belgian part of the North Sea where methane concentrations up to 1128 nmol L^{-1} were found. This value is not much lower than those measured at the UKCS blowout site UK22/4b (1450 µmol L^{-1}) and seeps at the Dogger Bank (1628 nmol L^{-1}) (Rehder et al., 1998; Mau et al., 2015). For comparison, the background concentration for methane in seawater of the North Sea in equilibrium with air is 2.5 - 3 nmol L^{-1} (Bange et al., 1994; Rehder et al., 1998).

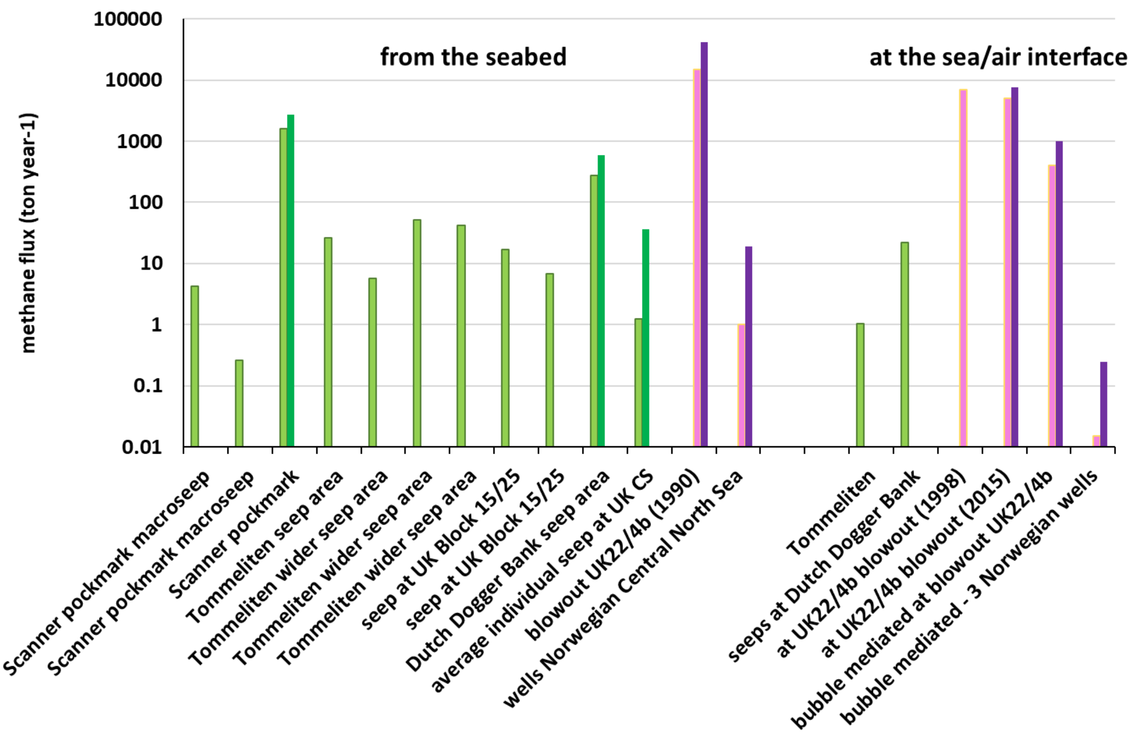

Figure 13. Methane fluxes from natural seeps (in green) and associated with gas wells (in pink/purple) both from the seabed and directly induced at the sea/air interface as measured in the North Sea. When two bars are denoted for one site, a range of values is valid where the lighter colour refers to the lower value and the darker colour to the higher one. See Table 3 for references for obtained data.

Table 3: Literature data on methane fluxes in the North Sea as based on measurements at individual sites for both natural seeps and well leakage.

site	no. seeps/wells	size	unit	flux	unit	CH4 flux (ton y-1)	remarks	reference
natural seepage out of seabed								
Scanner pockmark macroseep	120 seeps	100	m in diameter	24	m3 gas day-1	4.2	thermogenic source	Hovland & Sommerville, 1985
Scanner pockmark macroseep				1	m3 gas day-1	0.262	presumably erroneous value; should be 24 m3 day-1	Hovland et al., 2012
Scanner pockmark West		200-300	m in diameter			1600-2700		Li et al., 2020
Witch Ground Basin	> 1500 pockmarks	225	km2				many pockmarks not active; class I connected to deep biogenic CH4 sources; class 2 (99.5%) sourced by compaction-related	Bottner et al., 2019
Witch Ground basin							different associations for shallow gas	Fyfe et al., 2003
Norwegian Channel	pockmarks present in						gas at shallow depth in parts	Fyfe et al., 2003
Tommeliten seep area	five ebullition areas identified; 550 vents in	140000	m2	1.5 10^6	mol y-1	26.3	thermogenic; underlying salt diapirs	Schneider von Deimling et al., 2011
Tommeliten wider seep area	120 bubble streams	120000	m2	47	g m-2 y-1	5.64	thermogenic (Fyfe et al., 2003); above a subsurface salt dome	Hovland et al., 1993
Tommeliten wider seep area	120 vents	6500	m2	24	m3 day-1 at 75 m d	51		Hovland & Sommerville, 1985
Tommeliten wider seep area	120 seeps	6500	m2	6400	g m-2 y-1	41.6		Judd 2004; recalculated from Hovland & Judd
seep at UK Block 15/25		700x450	m in ovoid				probably thermogenic; three shallow reservoirs on top of each	Hovland & Sommerville, 1985
seep at UK Block 15/25		640000	m2	26	g m-2 y-1	17		Hovland et al., 1993
seep at UK Block 15/25		22825	m2	300	g m-2 y-1	6.8		Judd, 2004 (flux from Clayton & Dando, 1996)
northern Netherlands North Sea sector	pockmarks; seepage	2-10395	vppm CH4				biogenic and indicative thermogenic; salt structures play a role	Schroot et al., 2005
Dutch Dogger Bank seep area	850 flares within 8 km2	15000	m2	277	L min-1	273-593	five flare clusters, two of which predominant; predominantly	Romer et al., 2017
German Entenschnabel area (nw GCS)	minimum 166 flares	65	km2				flare observations not related to gas well sites; salt diapirism	Romer et al., 2021
northern, Norwegian North Sea		0.1-500 and 500->100000	ppb methane in head space				biogenic and secondary petroleum derived methane; major source: shallow marine sediments	Brekke et al. 1997
Belgian coastal zone (< 15km)		139	nmol L-1 on average in surface water				source: shallow peat-rich layer	Borges et al., 2016
Belgian coastal zone	shallow gas with no evidence of escape from						assumed biogenic; source: peat-rich layer or muddy marine sediments	Missiaen et al., 2002
German Bight pockmark field	up to 1200 pockmarks km-	915	km2	5000	ton in 3 months	abrupt emergence	suggested biogenic; source: shallow Pleistocene, fluvial	Kramer et al. 2017
anthropogenic leakage								
blowout UK22/4b (1990)	5 major plumes	20x18	m ellipse			15000 - 41000	thermogenic	Leifer, 2015
blowout N2/4-14 (1989)	3.3 Mm3 gas at 830 m depth	0.1-15	m3 of gas present				thermogenic; lateral migration at depth; episodic flow at shallow depth	Landro et al., 2019
Norwegian Central North Sea	3 abandoned wells					1, 4 and 19	values for 3 wells; biogenic; one through seismic chimney	Vielstadte et al., 2015
UK Central North Sea	43 decommisioned wells						28 wells; release of likely primarily biogenic gas; shallow gas in	Bottner et al., 2020
sea/air flux - natural								
Tommeliten				10.8	nmol m-2 s-1	< 1.04		Schneider von Deimling et al., 2011
seeps at Dutch Dogger Bank		8	km2			21.7		Romer et al., 2017
zone along Dutch coast				0.6 - 60	nmol cm-2 day-1			Scranton & McShane, 1991
sea/air flux - man-induced								
at UK22/4b blowout		10000	km2	1.2 E6	mol day-1	7008		Rehder et al., 1998
at UK22/4b blowout						< 5000-7500		Gerilowski et al., 2015
bubble mediated at blowout UK22/4b						700 ± 300		Schneider von Deimling et al., 2015
bubble mediated - 3 Norwegian wells	3 abandoned wells					0.015, 0.016 and 0.250	only emission from gas bubbles considered	Vielstadte et al., 2015

Table 4: Literature data on total methane fluxes as calculated for the entire North Sea, parts of it or associated estuaries.

site	no. seeps/wells	size	unit	CH4 flux (ton/y)	remarks	reference
natural seepage out of seabed						
UK cont. shelf - upscaling	173003 seeps	600000	km2	216000 - 6200000	upscaling; total of seeps at the UKCS	Judd et al., 1997
UK cont. shelf - upscaling		600000	km2	87000 - 2900000	upscaling; total of seeps at the UKCS	Tizzard, 2008 in Judd, 2015
total natural seepage from seabed at the North Sea		570000	km2	200	from literature refs	Vielstadte e.a., 2017
anthropogenic leakage						
North Sea - upscaling	11122 active and inactive wells	570000	km2	3000 - 17000	shallow biogenic gas leaking; upscaling via 2000 km2 area with probability of 18 out of 55 wells leaking	Vielstadte et al., 2017
UK Central North Sea - upscaling	1792 decommisioned wells	20000	km2	700-4200	100% of wells within < 300 m shallow gas pocket	Bottner et al., 2020
surface water/surface water						
production at Rhine estuary				7640		Upstill-Goddard et al., 2000
CH4 flux from North Sea to Atlantic Ocean				7569		Rehder et al., 1998
sea/air flux - natural						
estuaries in UK				5800 ± 5800		Upstill-Goddard & Barnes, 2016
Rhine estuary				7200		Upstill-Goddard et al., 2000
UK cont. Shelf - upscaling	associated with seeps			10000 - 480000		Tizzard, 2008 in Judd, 2015
UK cont. Shelf - upscaling	173003 seeps	600000	km2	119000 - 3400000		Judd et al., 1997
zone along Dutch coast - integration		~130x20	km2	90-9000	Methane source probably Rhine and Scheldt rivers	calculated from Scranton & McShane, 1991
North Sea - sea/air flux - model1		575000	km2	7543	entire North Sea - model 1	Bange et al., 1994
North Sea - sea/air flux - model2		575000	km2	5803	entire North Sea - model 2	Bange et al., 1994
North Sea - sea/air flux		575300	km2	24000 - 50000	entire North Sea	Rehder et al., 1998
sea/air flux - man-induced						
leakage along oil/gas wells - upscaling	11122 active and inactive wells			1000 - 7000		Vielstadte et al., 2017

Table 3 also illustrates that the methane released may be thermogenic and biogenic. The first indicates that hydrocarbon reservoirs are the primary source. Salt diapirism is found to play a major role here. The second indicates shallow gas where the sedimentary environments vary: marine sediments, peat-rich layers or Pleistocene fluvial sediments as indicated in *Table* 3.

As indicated in *Table 4*, the rivers that flow into the North Sea and the associated estuaries are sources of methane as well, such as the Wadden Sea along the Dutch, German and Danish coast (Scranton & McShane, 1991; Rehder et al., 1998; Upstill-Goddard et al., 2000). Methane concentrations in the order of tens of nmol L^{-1} are not uncommon in estuaries, where a correlation can be present with the salinity (Upstill-Goddard et al., 2000). Such concentrations are an order of magnitude larger than the background concentration. In the estuaries and the Wadden Sea, the intertidal and supratidal flats are a major source of natural methane. The methane production associated with the Rhine is substantial with 7640 tonnes/year. The accompanied atmospheric emission to air is also substantial so the net contribution to the North Sea is around 440 tonnes y^{-1}. The methane flux from the North Sea to the Atlantic Ocean is estimated at 7,569 tonnes y^{-1} and thus is an important sink.

Table 3 presents emissions of methane from sea to air, too. Most of the presented values for the individual sites equal several thousand to 20,000 tonnes y^{-1}. It is striking that the sea/air emission at Tommeliten is estimated as < 1.04 tonnes y^{-1} whereas the flux from the seabed is estimated as 26.3 tonnes y^{-1} (Schneider von Deimling et al., 2011). This indicates that most of the methane is lost in the water column. Comparably, the sea-air flux for the Dutch Dogger Bank is 21.7 tonnes y^{-1} whereas that at the seabed is 275-593 tonnes y^{-1} in the same study (Romer et al., 2017). Both seep sites are in relatively shallow water which illustrates that the decrease from seabed to sea surface can be strong for natural seeps in shallow marine waters.
Five records are presented for the emission of methane out of the North Sea or the UKCS to air. Strikingly, the values for the UKCS are higher than for the entire North Sea which appears inconsistent. Four of the records are from studies in the 1990s so more actual data is desirable. As with the data for the natural seepage across the UKCS, the more recent study by Tizzard (2008) provides a lower range than the older study by Judd et al. (1997).

An aspect that deserves attention is aerobic methane oxidation (in the water column). Mau et al. (2015) report oxidation rates from 0.04 to 840 nmol day^{-1} at seeps in the Dutch Dogger Bank, so from negligible to very high. The median rate was 4.0 nmol day^{-1} for the summer season and 0.2 nmol day^{-1} for the winter season. Based on this, Mau et al. (2015) claim that lateral discharge of methane from seeps and associated dilution by dispersive mixing are the major attenuation mechanisms whereas the effect of aerobic methane oxidation is small. In principle, this may hold for both methane from natural seeps and methane from leaking wells as long as the supply from the seabed is comparable in terms of bubble rate and size, etc.

4.4 Human-induced leakage

11,112 wells were present in 2012-13 in the North Sea excluding sidetracks and multilateral wells (Vielstädte et al., 2017). 2818 of these were active (i.e., producing or injecting) at that time. The integrity of offshore wells has been addressed at national level as summarised by Davies et al. (2014). *Table 5* presents the findings for offshore Norway and UK where it must be realised that not all Norwegian wells may be located in the North Sea. Based on these data, it concluded that well integrity issues are not uncommon for these wells, but this cannot directly be linked to active well leakage. Measures taken may prevent this.

Table 5: Statistics on barrier failure and well integrity failure for offshore Norway and UK as summarised by Davies et al. (2014) and consultation of the website for the UK study.

No. wells studied	% Wells with barrier failure or well integrity failure	Additional information	Source provided
Norway			
193	38	Abandoned wells, drilled 1970-2011. Well integrity and barrier failure. 2 wells with likely leak to surface.	Vignes (2011)
217	25	Wells monitored 1998-2007. Well integrity and barrier failure. 32% of the leaks occurred at well head.	Randhol & Carlsen (2007)
711	20	Barrier failure	Nilsen (2007)
406	18	Wells drilled 1977-2006. Well integrity and barrier failure. 1.3% had well head failure.	Vignes & Aadnoy (2010)
UK			
3167	10	10% shut-in during the last five years (as in 2005) as a result of ‘structural integrity issues’	https://www.ogj.com/drilling-production/article/17244448/otc-aging-uk-wells-have-structural-integrity-problems

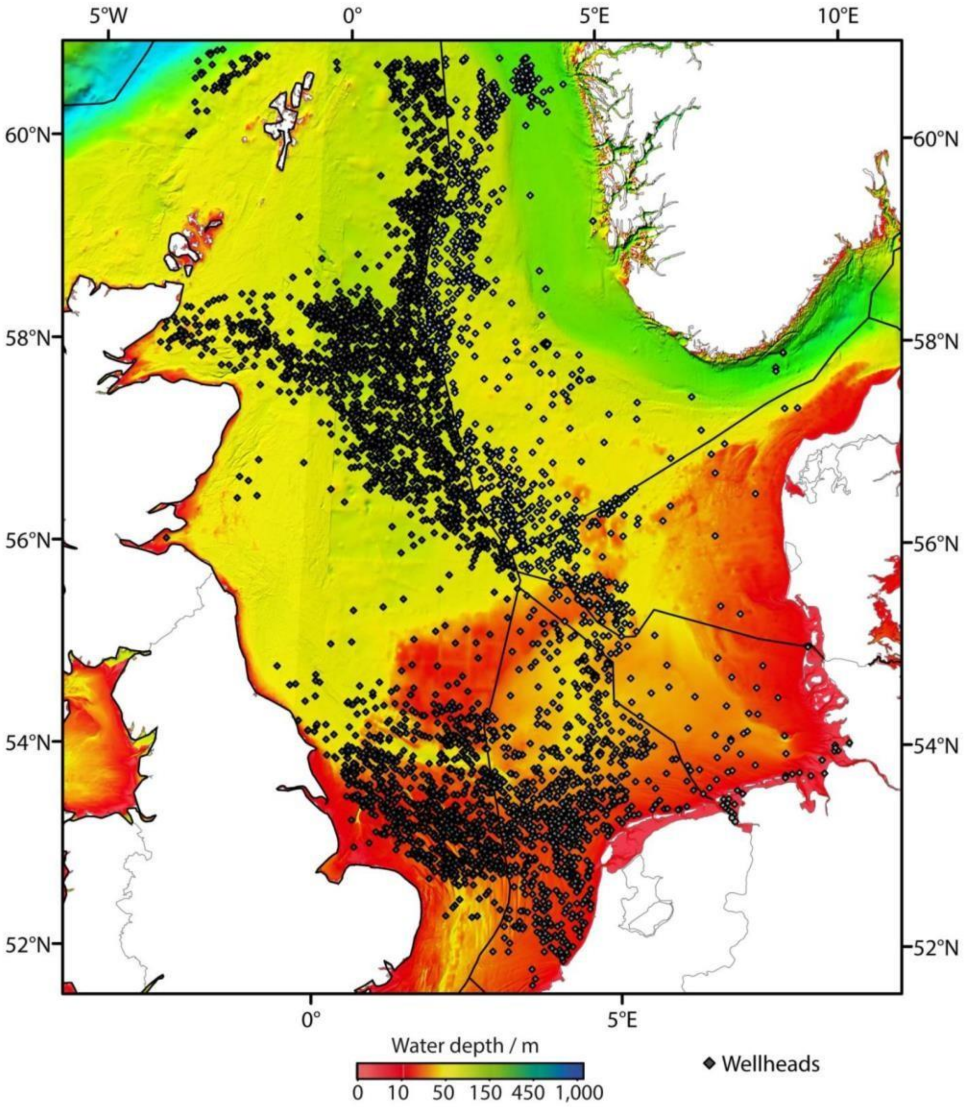

Figure 14: Bathymetric map of the North Sea with surface locations of the 11,122 wells (derived from Vielstädte et al. (2017).

A series of studies addressed leakage of gas at gas wells in the North Sea (*Table* 3). Several articles are devoted to the blowout at UK well 22/4b (in the literature referred to as UK22/4b) that happened in 1990. This blowout provides the largest release of methane at an individual site in the North Sea: 15,000 – 41,000 tonnes y^{-1} from the seabed (c. 90-96 m depth) in 2011. The associated direct release to air is <5,000 - 7,500 tonnes y^{-1}, part of which is via gas bubbles. In an earlier investigation published in 1998, this was quantified as 7,008 tonnes y^{-1}. Part of the leakage presumably disappears in lateral direction by seawater flow. The above numbers indicate that the release has not decreased substantially in time as concluded by Leifer et al. (2015), so the gas reservoir has not fully depleted since the 1990 event. The leakage varies in time at short (minutes) and longer (days/years) time scales where elastic behaviour is observed inducing eruptions. Three more blowouts are known for the North Sea. In 1980, Norwegian well 34/10–10 had a blowout from a reservoir located 230 m below seafloor (Hovland, 2007). There was another blowout at Norwegian well 2/4-14 in 1989, which was investigated recently by Landro et al. (2019). The underground gas blowout lasted for almost a year after which it was stopped by a relief well.

Released gas continued to flow to the shallow subsurface and probably continues until now. Another blowout happened in the early stage of gas exploration at the North Sea during an explorative drilling in the German Bight (Nordsee B1; Kornfeld, 1964; Thatje et al., 1999). A successful effort was made to kill the well using heavy mud and cement. Unfortunately, no flux measurements are known for these three blowout sites, so it is unknown whether these sites still leak natural gas.

Vielstädte et al. (2015) quantified methane leakage at three abandoned wells in the Norwegian Central North Sea. All three wells targeted the Paleocene Heimdal Formation. One well was permanently plugged and abandoned as a dry well, while the other two boreholes proved gas in the Heimdal Formation but were subsequently plugged and abandoned. The calculated fluxes were 1, 4 and 19 tonnes y^{-1}. The source was considered to be shallow, biogenic gas and flow was assumed to be occurring along the outside of the abandoned well and not through the well itself. The largest flux was found at a well that was drilled through a bright spot with a seismic chimney above the seismic anomaly. The lowest flux was found at a well where there was a bright spot but no seismic chimney. The intermediate value was found at the dry well where seismic layering was disturbed but without a seismic chimney.

Böttner et al. (2020) assessed 43 decommisioned wells in the UK Central North Sea that also includes the Scanner pockmark area. They found that 28 of these wells release gas, likely of biogenic origin, which is two thirds of the wells investigated. However, the possible presence of natural seepage around these wells was not accounted for whereas the studied area contains natural seeps as noted by Wilpshaar et al. (2021).

Both Vielstädte et al. (2017) and Böttner et al. (2020) performed upscaling calculations to estimate human-induced leakage of shallow gas along wells for either the entire North Sea (with active and inactive wells) or the UK Central North Sea (only decommisioned wells; *Table 4*). For the first situation, a total leakage from the seabed of 3,000 – 17,000 tonnes y^{-1} was calculated (Vielstädte et al., 2017) and for the second it was 700 – 4,200 tonnes y^{-1}. The first range is somewhat less than that for the blowout UK22/4b and 4-5 orders of magnitude smaller than the total natural seepage across the UKCS as estimated by Tizzard (2008). The latter volumes were noted earlier to be remarkably high. The associated emission of methane to the air was also estimated for the first situation as 1,000 – 7,000 tonnes y^{-1}. For comparison, this is about equal to or 1-3 orders smaller than other estimates on sea-air fluxes for the North Sea or UKCS (*Table* 3), where the maxima for the latter are remarkably high. It is slightly less than 1 promille of the oceanic emission of methane to air from geological sources (Table 1). The upscaling calculations by Böttner et al. (2020) and Vielstädte et al. (2017) were critised from the perspective of geosciences and well technology by TNO (2017, 2018) and Wilpshaar et al. (2021). The critique can be summarised as that both studies assume unproven and unlikely migration pathways for shallow gas in their upscaling while neglecting natural seepage of methane as alternative pathway at the North Sea. We refer to the original references for more extensive argumentations against the calculations made.
`

5 Gulf of Mexico

5.1 Introduction

The Gulf of Mexico is a passive margin basin that exists since Late Triassic times as a result of plate tectonic movements. It has been subsiding ever since and thick clastic wedges have been accumulating along the northwestern and northern margins of the Gulf of Mexico, particularly during the Cenozoic. It is a prolific oil and gas producing basin.

The Gulf of Mexico is also well known for its natural seeps of both oil and gas. These seeps have frequently been studied since 1970s but the number of studies that provide quantitative assessments of the fluxes is limited. Reference is often made to ''cold seeps'' in contrast to hot hydrothermal vents that can also be found in marine environments. In this literature study we have tried to collect those studies that provide quantitative data on methane fluxes related to natural seeps and human-induced leakage.

The Gulf of Mexico can be considered, on the basis of bathymetry, to be split in to three parts (Figure 15): first, the continental shelf that contains a broad zone west of Florida, south of Texas and Louisiana, and north of the Mexican provinces Campeche and Yucatan. Second, the continental slope that is extensive in front of the northern continental shelf and to the west of the Mexican shelf (and north of the Mexican province of Tabasco). Third, the abyssal plain that lies in the centre and almost reaches the eastern coast of Mexico.

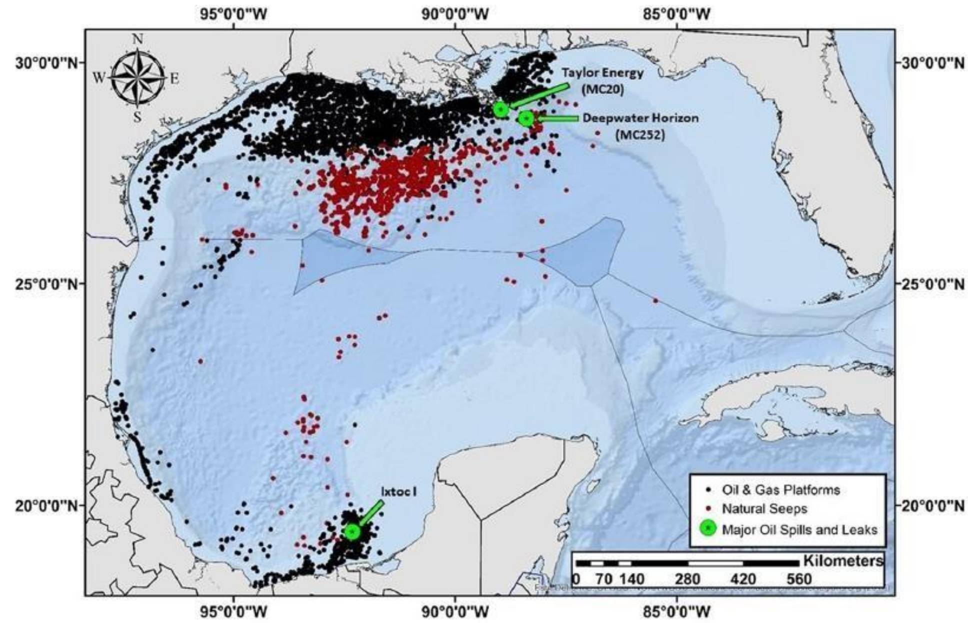

Figure 15: Surface locations of oil and gas platforms and natural oil seeps. The locations of three major oil-related spills are also indicated (derived from Pulster et al., 2020). The legend speaks of oil seeps where it holds that many oil seeps also release natural gas.

5.2 Geology

5.2.1 Oil and gas exploration

Oil and gas exploration in GoM dates back to 1901, when the Spindletop well blew out on the Gulf of Mexico coast near Beaumont, Texas. Following successful exploration onshore, the marine part of GoM was subsequently explored by drilling in ever deeper waters, starting in 1948. As of 2018, there were 2,024 platforms and 53,068 wells drilled at water depths varying from very shallow to over 2000 m (Rogener et al., 2018).

Oil and gas production figures (*Figure 16*) show that deepwater production took off in the early nineties. Gas production peaked in 1997 and has been decreasing ever since despite the relative increase in contribution from deepwater fields. But even these have seen a decline since 2003.

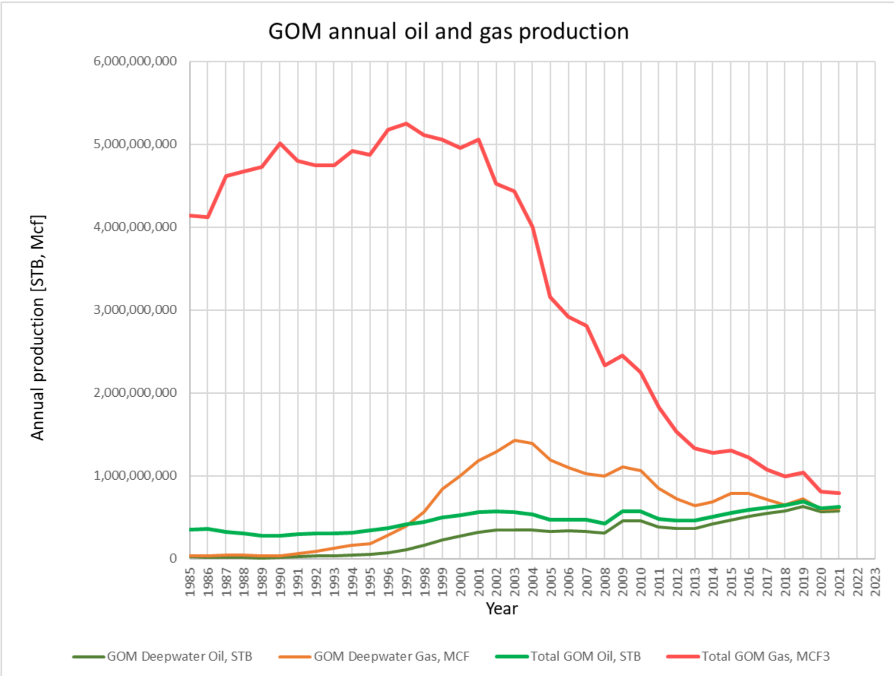

Figure 16: GoM oil and gas production. Data from BOEM.

Oil production is a different story. Although oil production seemed to have peaked in 2019, the slight decline in 2020 was mainly due to Covid. Production picked up again in 2021 and although the production in that year is still 8% less than in 2019, the peak in GoM oil production may not have been reached yet. In any case, over 90% of the oil is currently produced from deepwater fields (*Figure 16*).

5.2.2 Petroleum geology

The northern deep-water Gulf of Mexico is one of the most active deep-sea areas in the world for oil exploration and development. The geology of this area is complex, being dominated by multilevel allochthonous salt systems, normal and reversed faults, and large, salt-cored fold belts (Weimer et al, 2017). The occurrence of oil and gas fields in the deep-water GoM is intimately connected to this geological setting, as illustrated by *Figure 17* and *Figure 18*.
Figure 19 shows a north-south cross section through the northern GoM. Clearly visible are, apart from the 20 km thick sediment cover in the rift centre, the numerous salt bodies that give rise to

complex geological structures, which in their turn form traps and provide pathways for hydrocarbon migration. Weimer et al (2017) studied these salt bodies and their effects on the geological evolution of the area in detail. Most of what follows below is based on their work.
The Gulf of Mexico originated as a rift valley when North America started to move away from Africa and South America near the end of the Triassic. By the mid Jurassic, the rift valley became connected to the Pacific Ocean, and a thick package of evaporites, the Louann Salt, was deposited. Later, the upcoming Rocky Mountains provided enough detritus to form a thick sedimentary pile, up to 20 km thick, over the Louann salt. This thick sediment cover caused mobilization of the salt, thereby creating very complex geological structures (*Figure 20*). Salt bodies detached from the main salt layer at various points in time, moved upward and were emplaced as salt sills at various depths, often forming diapirs.

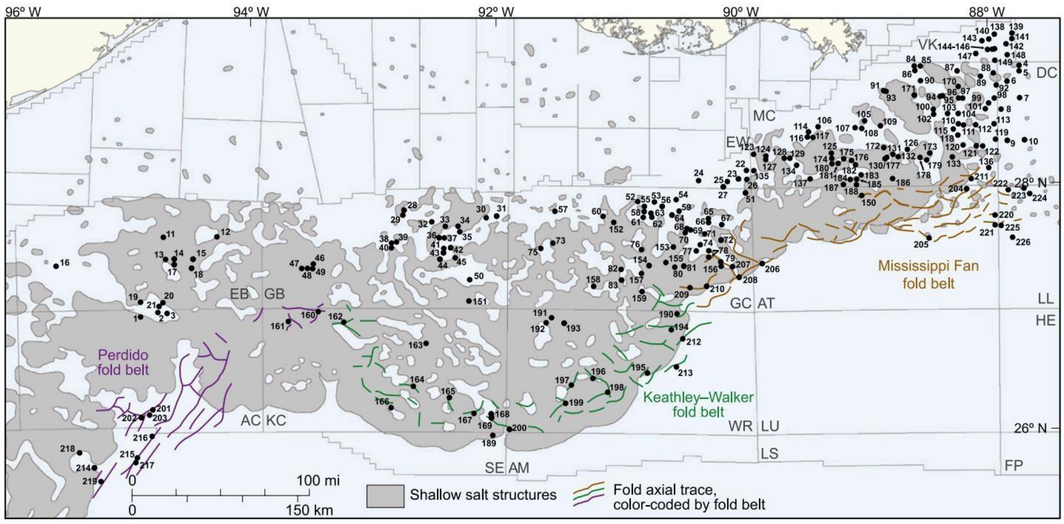

Figure 17: Regional map of the northern Gulf of Mexico showing the occurrence of shallow salt structures, locations of major structural features, and the 226 fields and discoveries (black dots) in greater than 1500-ft (457-m) water depth (Weimer et al, 2017).

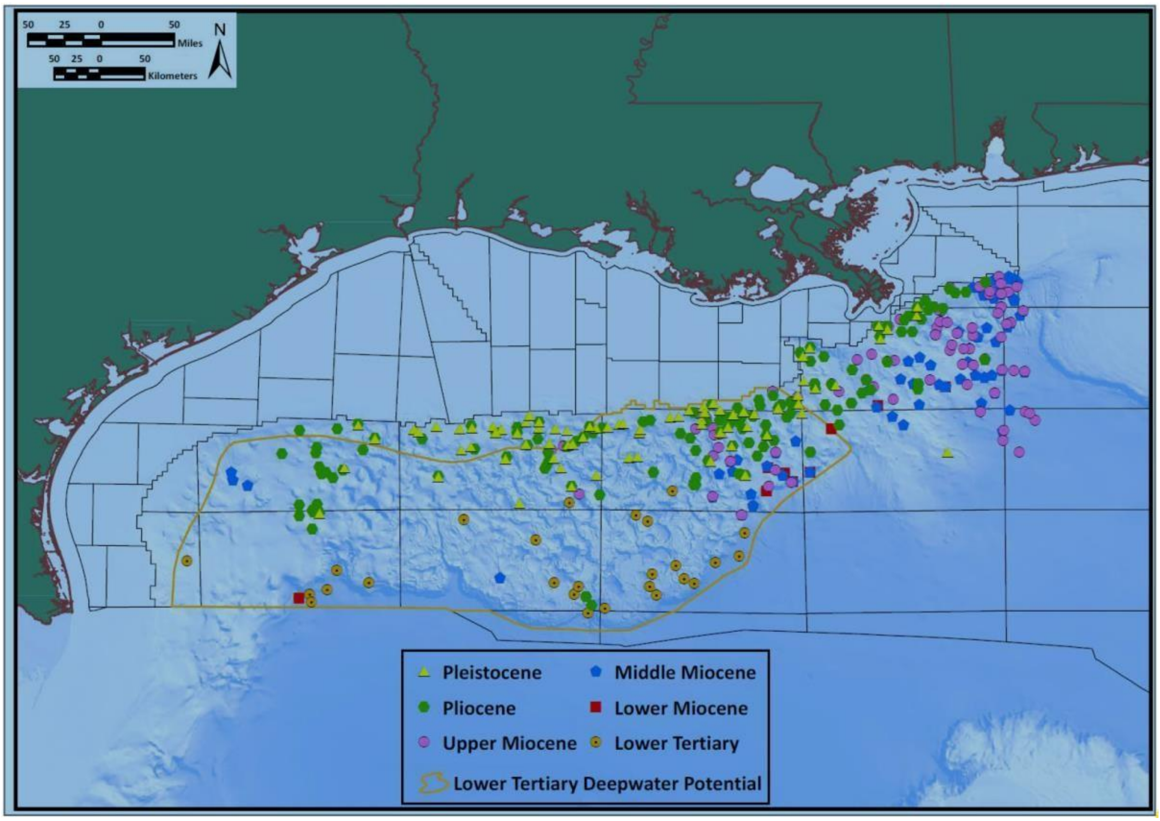

Figure 18: Geological age of deep-water GoM fields and discoveries (BOEM, 2017).

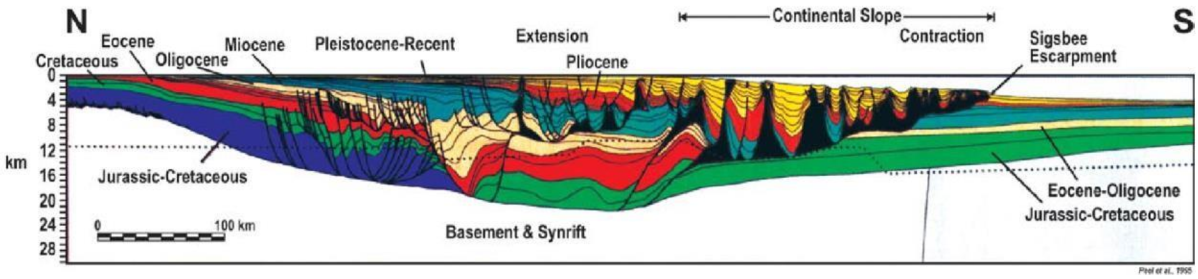

Figure 19: A north-south geologic cross section of the northern Gulf of Mexico basin illustrating the complex relationships between sediments and salt (black). From Peel et al. (1995) in Fisher et al. (2007).

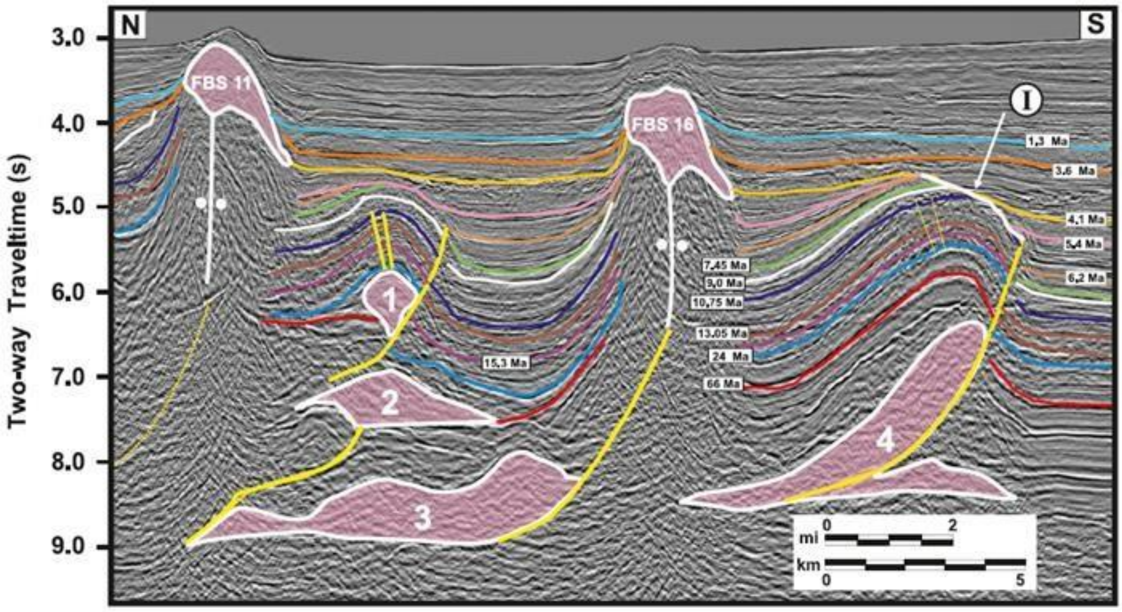

Figure 20: Example of the geological complexity created by salt mobilization. Salt bodies FBS 11 and FBS 16 are Neogene allochthonous salt bodies, whereas salt bodies 1 and 2 are emplaced during earlier stages: intra-Paleogene for salt body 1 and intra-Cretaceous for salt body 2. Salt bodies 3 and 4 are also likely allochthonous (Bouroullec and Weimer, 2017).

5.2.3 Source rocks and petroleum generation

The Gulf of Mexico is a sedimentary basin rich in source rocks. Nehring (1991) lists about 30 stratigraphic levels in the sedimentary record of the GoM that can be considered source rocks. For the major offshore hydrocarbon systems Hood et al (2002) reduced that number to three major source rock intervals: lower Tertiary (centered on Eocene), Upper Cretaceous (centered on Turonian), and Upper Jurassic (centered on Tithonian). *Figure 21* shows the Mesozoic source rock intervals as well as some reservoirs of the same age.

Oil and gas generation took place at various times for the different source rock intervals. In general, it can be said that the younger the source rock, the later the timing of oil and gas generation. However, there are exceptions to this rule.

Figure 22 shows an example where a Tithonian source rock started to generate oil in the Paleocene, earlier than an Oxfordian source rock in the same area which only started oil generation in the Miocene. However, all source rocks have peak oil and gas generation in the Tertiary.

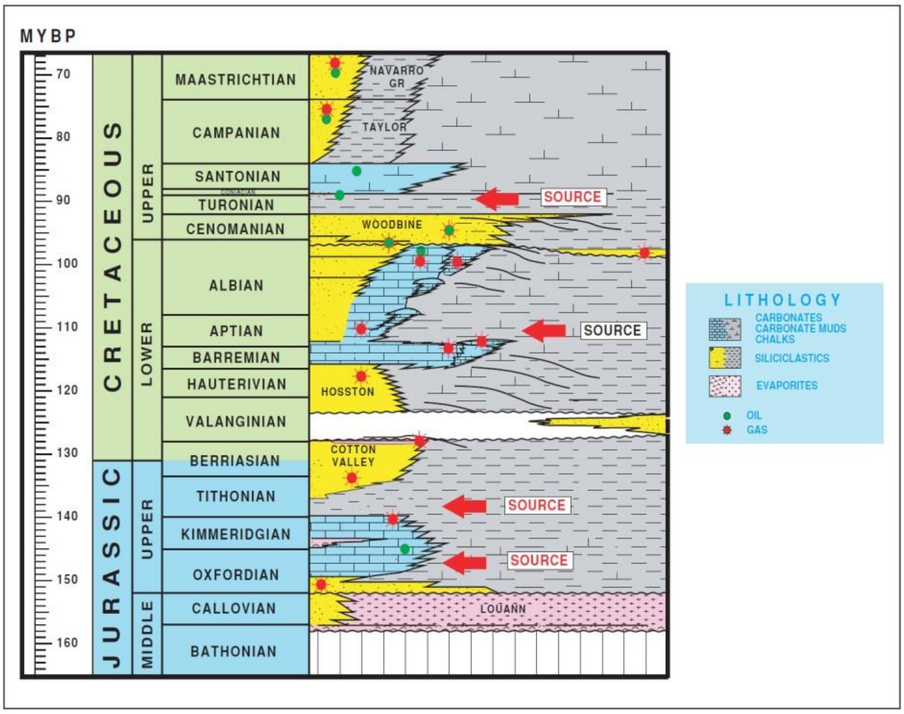

Figure 21: Stratigraphic column showing the Mesozoic source intervals (arrows) for the offshore Gulf of Mexico (Hood et al, 2002).

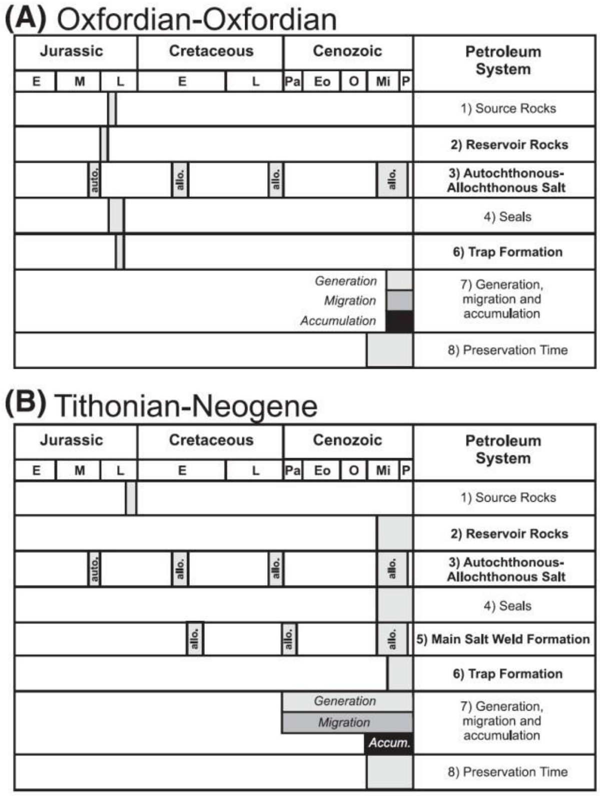

Figure 22: Petroleum systems element charts showing the timing of main elements for an area near the Mississippi Canyon (Bouroullec et al, 2017).

5.2.4 Migration pathways

In order to move hydrocarbons from deep source intervals to younger Tertiary reservoirs cross- stratal migration is required. Apart from a slow upward migration through the various formations (including shales), the creation of these migration pathways can be accomplished in two ways: faulting and salt movement. The Gulf of Mexico provides ample examples of both types of migration pathways.

Table 6. Literature data on methane fluxes in the Gulf of Mexico as based on measurements at individual sites for both natural seeps and well leakage.

site	no. seeps/wells	flux	unit	CH4 flux (ton y-1)	remarks	reference
natural seepage out of seabed						
continental shelf - northwestern Go	14 seep sites at 3-30 m depth only	< 0.001 to > 50	L min-1	up to > 37	11 microbial and 3 thermocatalytic; C1/(C2+C3) ratio as	Bernard et al., 1976
Birthday Candles		3.2 - 8.2 E5	mol y-1	9.12		Johansen et al., 2020
Mega Plume		3.2 - 5.2 E5	mol y-1	6.72		Johansen et al., 2020
brine seeps with advection	2 seeps	2 - 58	mol m-2 y-1		mixed bio/thermogenic or oxidized biogenic	Lapham et al., 2008
Green Canyon 185 (Bush Hill; 525-55	steady, pulsing and oily (man-induced!) pl	53.2, 7.55 and 1.64	mmol s-1	0.83 - 26.8	thermogenic gas; bubble characterisations	Leifer & MacDonald, 2003
Bush Hill (540 m depth)	gas hydrate mound + gas vents (c. 30000 m	5.2E+06	mol y-1	83		Solomon et al., 2008
northern cont. slope	6 plumes at 3 seep sites (incl. BH)	197 - 6520	µmol m-2 day-1		averages per site	Solomon et al., 2009
MC 118 Sleeping Dragon	entire vent at 890 m depth	0.2 - 0.3	L min-1	8.7 - 13		Wang & Socolofsky, 2015
MC 118 Woolsey Mound	883 m depth	2.0 ± 0.4	g s-1	36	gas contains 68.7 mol% CH4	Wang et al., 2020
MC 118 Woolsey Mound	75 cores studied	up to 754-2823	µmol m-2 day-1		thermogenic; highest fluxes associated with faults	Wilson et al., 2014
Alaminos Canyon block 601	brine pool 250 m diameter at 2334 m depth	1.1 ± 0.2	mol m-2 y-1	0.9		Wankel et al., 2010
Pascagoula, Biloxi and Gloria Domes	seeps at appr. 1130, 1380, and 1570 m dept	0.02 - 0.9	m3 day-1 (at depth)	up to 39.5	gas flux estimates with rough assumptions	Weber et al., 2013
Pascagoula Dome	1 seep	3.1E-06	m3 s-1	10.0	acoustic method; based on p.V = Z.n.R.T	Weber et al., 2014
Pascagoula Dome	1 seep	2.0-2.3E-6	m3 s-1		gas sampling method	Weber et al., 2014
Tsanyao Yang Knoll; southern GoMx	32 flares; 3400 m deep; part of Campeche K	8300 - 70600	mol h-1	1,163 - 9,895	gas bubbles almost entirely dissolve in water column; CH4 drops within 100 m above seabed	Romer et al., 2019
human-induced leakage at seabed						
Deepwater Horizon blowout		146-200	kton		during first 83 days after blowout	Kessler et al., 2011 + refs
sea-air fluxes - natural seeps						
northern cont. slope	6 plumes at 3 seep sites (incl. Bush Hill)	-0.38 - 7.0	µmol m-2 day-1		averages per site	Solomon et al., 2009
MC 118	6 sites at 900 m depth	0.744 - 300	mol day-1	0.0043 - 1.8	thermogenic	Hu et al., 2012
GC 600	1250 m depth	51.9	mol day-1	0.303	thermogenic	Hu et al., 2012
GC 185	550 m depth	6.85	mol day-1	0.0400		Hu et al., 2012
sea-air fluxes - human-induced						
Taylor Energy platform, MC 20 block	sea-air flux (crater diameter 10 m at 135 m	0.8	ton day-1	292	before oil containment	Silva et al., 2022
Deepwater Horizon	survey in June 2010	22.6	mol day-1	0.362 kg day-1	0.0303 ton during first 84 days after blowout	Yvon-Lewis et al., 2011
Deepwater Horizon	2 air-borne surveys in spring 2010	no enhancement above background			during initial containment and clean-up operation	Ryerson et al., 2011

5.3 Natural seeps

On a general note, it has been found that natural seepage in the northern Gulf of Mexico is more extensive at the continental slope than at the continental shelf (Kennicut, 2017). Here, over 90 seep sites from 290 to 3300 m deep were visually identified on the slope until 2007 (Fisher et al., 2007).

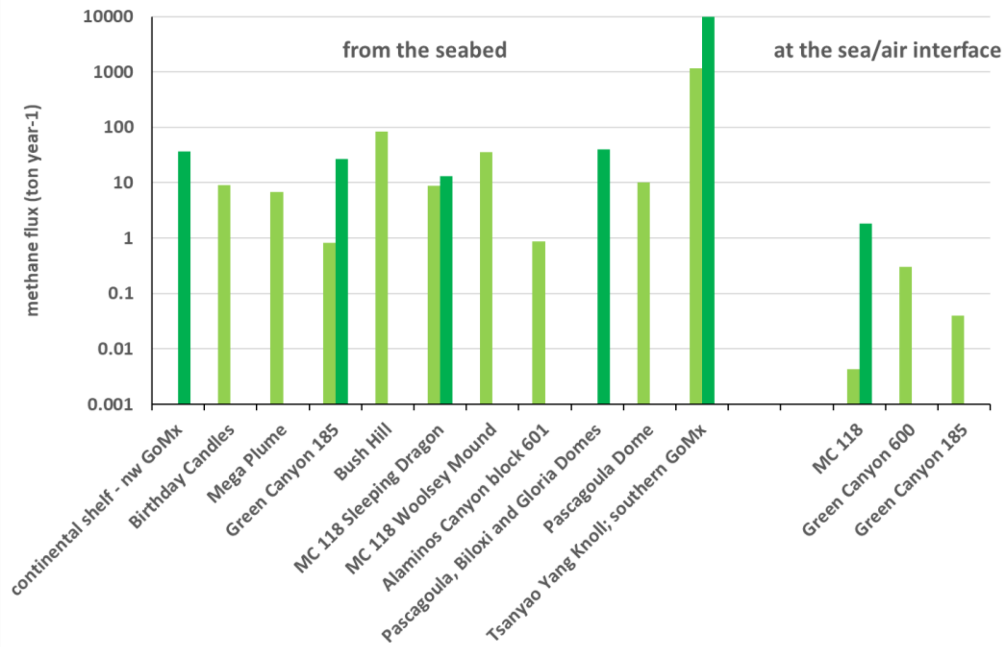

Figure 23. Methane fluxes from natural seeps both from the seabed and directly induced at the sea/air interface as measured in the Gulf of Mexico. When two bars are denoted for one site, a range of values is valid where the lighter color refers to the lower value and the darker color to the higher one. See Table 6 for references.

Table 6 summarises literature data on natural seepage and man-induced leakage at the Gulf of Mexico. Figure 23 graphically present the annual fluxes for the natural seeps; the studies on human-induced leakage were not included as the fluxes for Deepwater Horizon are no annual fluxes but incidental ones. The data indicates that the natural seep rate at individual sites lies between 1-10 tonnes y^{-1}. Most sites refer to the northern continental slope. Bernard et al. (1976) studied seeps on the continental shelf and found that most of them have biogenic gas and only 1 or a few thermogenic. The maximum flux of > 37 tonnes y^{-1} is substantial and compares well with seep fluxes in the North Sea. An exception is the seep field at Tsanyao Yang Knoll in the southern Gulf of Mexico. This field contains 32 flares and the integrated methane flux is high with 1,163 – 9,895 tonnes y^{-1}.

An impression on the total areal flux is obtained from Weber et al. (2014) who investigated an area of 6,000 km^2 in the northern Gulf where 357 seeps were found. The total methane flux for that area was calculated as 400 – 50,000 tonnes y^{-1} (Table 7). This is grossly equivalent to 1‰ of the global marine seepage from the seabed as estimated at 8 - 65 Mtonnes y^{-1} by the US-EPA (2010). One can also calculate from the range that the average methane flux per seep equals 1 – 140 tonnes y^{-1}. This upper value is high compared to values presented in *Figure 23*.

As briefly indicated in Chapter 3, a series of processes may be active at seep sites that cause a lowering of the methane flux from the deeper subsurface to the water column. This is well illustrated by Johansen et al. (2020) who present a mass balance approach on the methane sequestration around the seabed (Figure 24). Two major sinks in the shallow subsurface are production of gas hydrate resulting into the typical seabed ''mounds'' and anaerobic methane oxidation. Johansen et al. (2020) indicate that the flux may be diminished by several orders of magnitude by these two processes. As generally recognised, gas hydrates play a major role as a sink in the deep Gulf of Mexico. Gas hydrates are also found to contain thermogenic methane (Pohlman et al., 2005). Figure 25 presents a map in which part of the northern continental slope gas hydrates are assumed to be present. It should be noted that the blue area in the map shown is only where the hydrate resource has been assessed. Conditions for hydrate stability will naturally be present to the south of the area shown and into deeper water than was assessed by Milkov & Sassen (2002). Methane may be released to the water column via several pathways which is also illustrated in Figure 24.

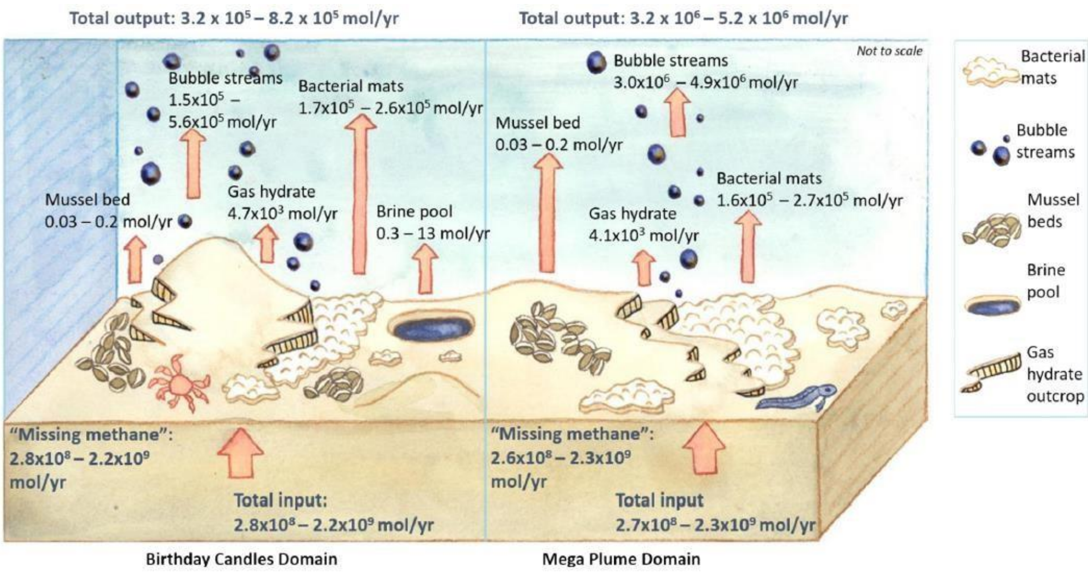

Figure 24: Illustration of the methane fluxes at the seeps Birthday Candles and Mega Plume (derived from Johansen et al., 2020.)

Table 7. Literature data on total methane fluxes as calculated for parts of the Gulf of Mexico.

area	no. seeps/wells	CH4 flux (ton y-1)	remarks	reference
natural seepage out of seabed				
northern Gulf of Mx (6000 km2)	357 seeps between 900-2600 m depth	400 - 50,000	integrated areal gas flux per seep	Weber et al., 2014
sea-air fluxes - natural				
northern continental slope	assuming 1500 - 5000 deep seeps	3000 - 9000	upper limit assuming maximum value of 1.75 ton y-1	Hu et al., 2012

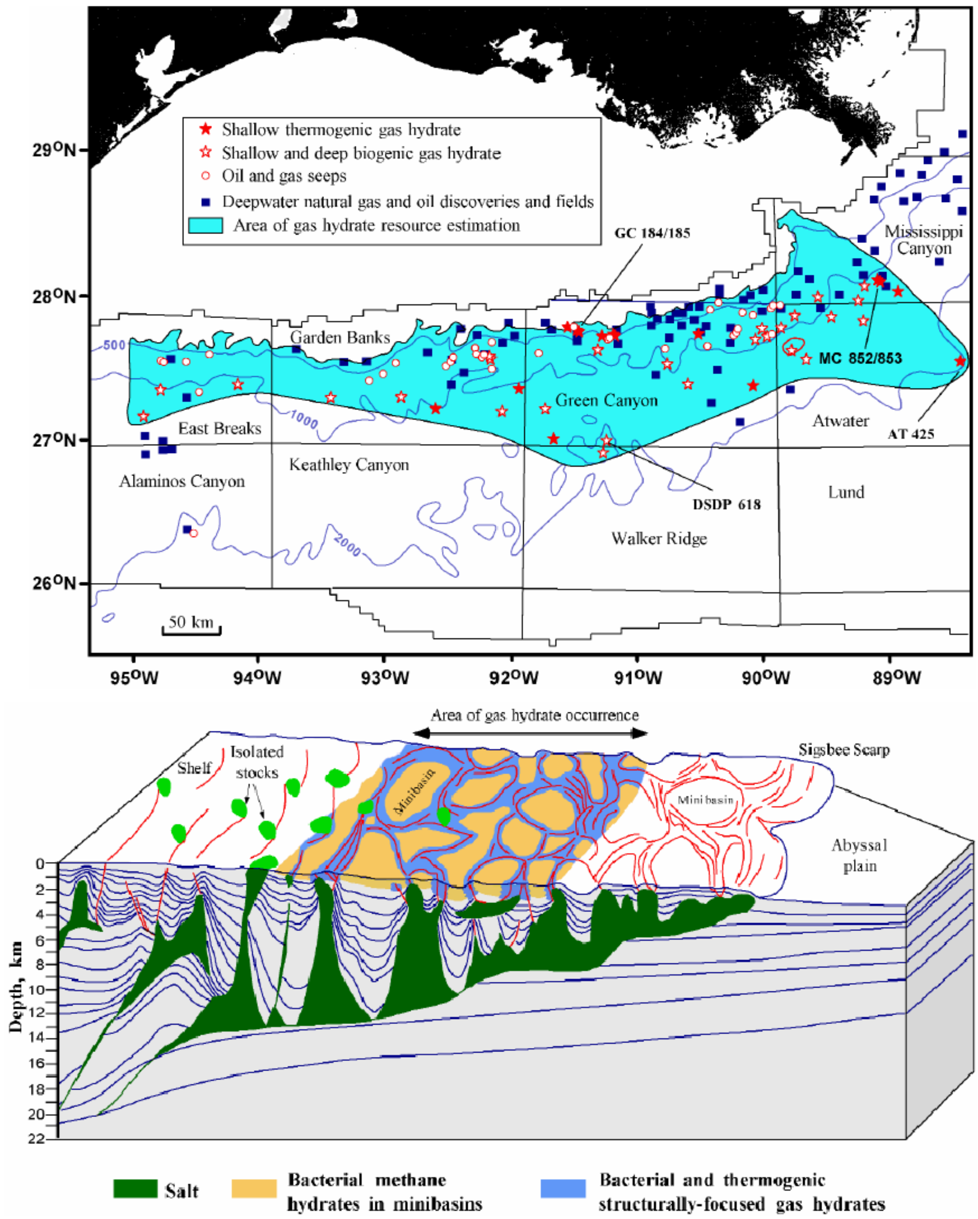

Figure 25: Map of northern Gulf of Mexico with indication where gas hydrates may be found as associated with seeps of natural gas (above) and their geological association with the salt diapirism (below; derived from Milkov & Sassen (2001).

Several studies present methane concentration depth profiles above seeps or profiles of bubble plumes in the GoM. For deepwater seeps, it is common that the bubble plumes do not reach the sea surface but disappear tens to several hundreds of meters above the seep site (e.g. Jerram et al., 2015; Leonte et al., 2018). Jerram et al. (2015) found for 161 plumes originating from 1400 m depth that most plumes terminated between 800 – 1100 m depth, several between 500 – 600 m and the rest with 360 m as a minimum depth of determination. A similar pattern is shown in *Figure 26* for another study at Tsanyao Yang Knoll in the southern Gulf of Mexico (Romer et al., 2019).

The situation can be different for shallow seeps on the continental shelf: Sassen et al. (2003) observed that gas bubbles are generated from a diapiric mud mound in Ship Shoal Block 286 at a depth of 80 m and probably reach the sea surface. This gas had a mixed thermogenic and biogenic origin.

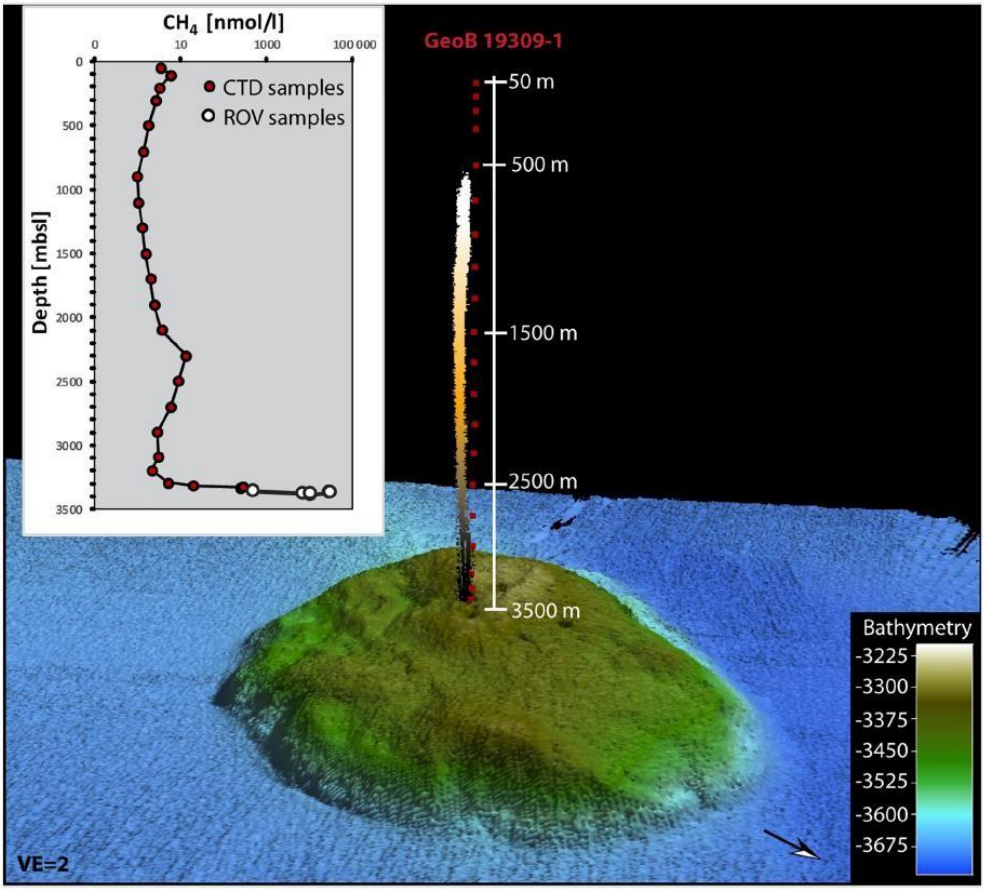

Figure 26: Bathymetry of the Tsanyao Yang Knoll seep with illustration of the fate of gas bubbles and in the inset concentration depth profile of the methane concentration (derived from Romer et al., 2019).

Table 8 summarises data on aqueous methane concentrations at seeps and in the water column. For reference: seawater in equilibrium with the atmosphere contains about 2.2 nmol L^{-1} in the Gulf of Mexico. The data indicate that the methane concentration lies far above 1000 nM when sampling is undertaken very close to a major seep. It is typically found for deep seeps that the aqueous methane concentration drops several orders of magnitude within the first tens of meters above the sea floor due to dispersion in seawater (*Figure 26*). The study by Leonte et al. (2018) is an exception as they found large heterogeneity in time and also with depth. It should be noted that rapid dissolution from gas bubbles (when present) causes aqueous concentrations to rise and thus plays an opposite role to dispersive mixing. The importance of lateral seawater flow as an attenuation mechanism is well illustrated by Meurer et al. (2021) who performed detailed concentration mapping around the Bush Hill seep. Their data illustrates that elevated concentrations of around 100 nM to severals tens of nM are observed with increasing lateral distance from 0.5 to 2 km away from the seep site and within the first 30 m above the seabed.

Table 8. Summary of data on methane concentrations at natural seeps and at sites with human-induced leakage as observed in the Gulf of Mexico (note that seawater in equilibrium with the atmosphere contains about 2.2 nmol L^{-1} in the Gulf of Mexico).

site	background information	conc. near seep/spill	at shallow depth	unit	remarks	reference
natural						
cruise from cont. platform to abyssal plain	14 stations	> 30	15 - 25	ml methane L-1		Frank 1970
northern continental slope	8 different sites (near	up to 24-45	11 - 14	nM		Rakowski et al., 2015
brine pool Alaminos Canyon	2334 m depth	180,000 - 590,000	30	nM	24 - 111 µM close to pool	Wankel et al. 2010
Woolsey Mound (Mississippi Canyon 118)	900 m depth	400 - 40,000	30 - 400	nM		Leonte et al., 2018
Tsanyao Yang Knoll (southern GoMx)	3400 m depth	30,000	< 10	nmol L-1	5 - 13 nM up to 1000 m	Romer et al., 2019
Bush Hill	540 m depth	up to 400		nM	typically 50 - 100 nM laterally away from the seep	Meurer et al., 2021
eight seep sites at northern cont. slope	550 - 1250 m depth		1.75 - 23.5	nM		Hu et al., 2012
northern GoMx - 27 surveys	161 plumes				80% attenuation of bubbles between c. 1400 to c. 600 m depth; large temporal	Jerram et al., 2015
reference for Deepwater Horizon	31 sites and c. 900	up to 274		nM	expedition in 2001 visiting	Rogener et al., 2018
man-induced						
Taylor Energy platform; MC 20 block		up to > 60,000	2 - 70	nM		Silva et al., 2022
Macondo wellhead location + northern slope	May-June 2010	up to 381 ,000	< 1000	nM		Rogener et al., 2018
Deepwater Horizon plume	4-6 months after blowout when wellhead was	1.4 ± 2.0 (max 20.4)		nM		Kessler et al., 2011

The dispersive mixing of methane emitted from deep sites within the water column implies that the direct flux of methane to air will be strongly muted compared to that from the seabed. Aerobic oxidation of methane in the water column will be another attenuation mechanism although the oxidation rate close to the seep is observed to be considerably higher than higher up in the water column (Wankel et al., 2010).

As illustrated in *Table* 8, the methane concentrations at shallow depth (and in the photic zone) usually range up to a few tens of nM. This is well above the background concentration of 2 nM. An exception is the data by Leonte et al. (2018) where concentrations up to 400 nM were found at 100 m depth. As indicated in *Figure 27*, the methane concentration in the shallow, photic zone may be elevated by biological processes compared to the atmospheric equilibrium concentration. This was observed by Rakowski et al. (2015) where a typical range of 11-14 nM is found for shallow seawater, which is attributed to biological methane production. An important implication is that elevated concentrations at shallow depth cannot automatically be attributed to seeps (or external sources such as the Mississippi River as also seen for River Rhine; *Table 4*) and so the associated sea-air emissions.

A few studies have quantified the sea-air flux above seep sites as summarised in *Table 6*. The size of the flux varies almost three orders of magnitude, and the highest values lie in the lower range of the fluxes of seeps at the seabed. The data is for deep seeps at the continental slope and illustrates that a fraction of the flux at the seabed may reach the sea-air interface despite the considerable depth and attenuating processes in the water column.

Hu et al. (2012) also performed a straightforward upscaling calculation to estimate the total, direct methane flux from seeps to the atmosphere (*Table* 7). They assumed 1500 – 5000 deep seeps to be present across the US northern continental slope and calculated that the upper limit of the total flux is 3,000 – 9,000 tonnes y^{-1} using their maximum value of 300 mol day^{-1} as flux per site. The total flux would be three times lower for the observed average of 114 mol day^{-1} $site^{-1}$. Note that the fate of laterally discharged methane from seeps has not been researched and is thus unclear for the Gulf of Mexico.

5.4 Human-induced leakage

The Gulf of Mexico has been significantly impacted by oil and gas exploration and production. As of

2018, there were 2,024 production platforms and 53,068 wells drilled at water depths varying from very shallow to over 1000 m (Rogener et al., 2018). A limited number of studies that address well integrity issues and catastrophic events is publicly available.

According to Kaiser (2017) over 11,000 wells were plugged and abandoned in the U.S. part of the Gulf of Mexico. 502 of these wells at the continental shelf were tracked for 5 years for bubbling/leaking events. Nine of them required remediation. This gives a probability estimate of 1.8% with a 95% confidence interval of 0.6 – 3.0%. Another cited study speaks of 11,498 wells with integrity issues, 5459 were shut-in or temporarily abandoned and leakage was reported for 0.01 – 0.05% of them (i.e., 1-6 wells). Brufatto et al. (2003) came up with comparable numbers: 43% of 15,500 wells at the continental shelf have sustained casing pressure on at least one casing annulus with 26.2% of the barrier failures in the surface casing. Bernard (1976) sampled 4 vents at the northern continental shelf that are ''non-commercial byproducts of offshore petroleum production'', which suggests that they are man-induced. The vents produced petrogenic gas as indicated by analysis of light alkanes. We are not aware of scientific studies that assessed well leakage in a quantitative way as performed for the North Sea.

The occurrence of blowouts in the U.S. Outer Continental Shelf (OCS; which also includes areas outside the northern Gulf of Mexico) has been statistically studied by Skalle & Podio (1998) and Izon et al. (2007). The first reported that 35,000 wells were drilled between 1960 – 1996. The number of blowouts was 186 (0.53%) with 123 of them (0.35%) during drilling. The latter reported that 39 (0.26%) blowouts occurred during 1992 – 2006 when 15,077 wells were drilled in the OCS. They also reported that the blowout percentage was 0.41% for the period 1971-1991. The frequency thus went down with fewer fatalities and injuries, too. Izon et al. also stated that the environmental impacts were negligible. The influx of shallow gas was the major contributor to blowouts. The blowouts usually ceased either man-induced by pumping mud or cement, or naturally by sediment bridging or depletion of shallow, trapped gas. According to Izon et al., this makes it unlikely or less likely that long-term leakage occurs at these blowout sites.

Finally, three major catastrophic accidents are known at which a large amount of oil and associated methane was released from the subsurface:

- The Ixtoc-1 blowout in September 1979 in the southern Bay of Campeche (Soto et al., 2014);
- The Taylor Energy platform at the continental shelf that became destroyed by Hurricane Ivan in September 2004.
- The Deepwater Horizon blowout in April 2010 at Macondo at the northern continental slope; The methane chemistry has been scientifically addressed for the last two accidents as briefly summarised below.

The destruction of the Taylor Energy oil platform is a special event that lies outside the common scope when it comes to methane emissions (or other environmental impacts). The accident occurred in the aftermath of a hurricane when a storm-induced mudslide destroyed the platform to which 28 wells supplied oil and gas. The consequence was an oil leakage in excess of 4.5 m^3 day^{-1} during 2018. The associated emission of methane to the air was 0.8 tonnes day^{-1} (*Table 6*). This situation has lasted for 14 years so the total atmospheric emission was c. 4,088 tonnes assuming a steady spill flux. The shallow depth of the spill caused little attenuation of methane within the water column although the highest aqueous concentration of methane decreased from 70,000 nmol L^{-1} to less than 100 nmol L^{-1} at less than 30 m depth. The spill got contained in 2019 although it is still an active oil spill. The highest methane concentrations at 120 m depth were somewhat below 2000 nmol L^{-1} in 2021. This accident illustrates that ageing oil and gas infrastructure may be vulnerable to submarine landslides which are frequently observed in parts of the Gulf of Mexico (Maloney et al., 2019; Fan et al., 2020). One associated risk is leakage of oil and gas to the environment after such events.

The Deepwater Horizon (DWH) drilling rig suffered a blowout at 20 April 2010. The rig was operating above the "Macondo" wellhead on the upper continental slope in 1520 m of water. The well was capped after 84 days during which a large amount of oil and gas was released. The released amount of methane during this period is estimated to be 146,000 – 200,000 tonnes. Rogener et al. (2018) compared the methane plume from the DWH blowout to that of deep natural seeps. The methane concentration ranged up to 381,000 nM for blowout and post- blowout conditions with highest concentrations near the seabed (*Figure 27*). Concentrations up to 10,000 nM occurred up to 600-700 m depth and the concentration was below 1,000 nM near the surface. A major increase in methane oxidation activity was observed in response to the large methane input which lasted for multiple years after the blowout. Dispersive mixing also lowered the methane concentrations in addition to methane oxidation.

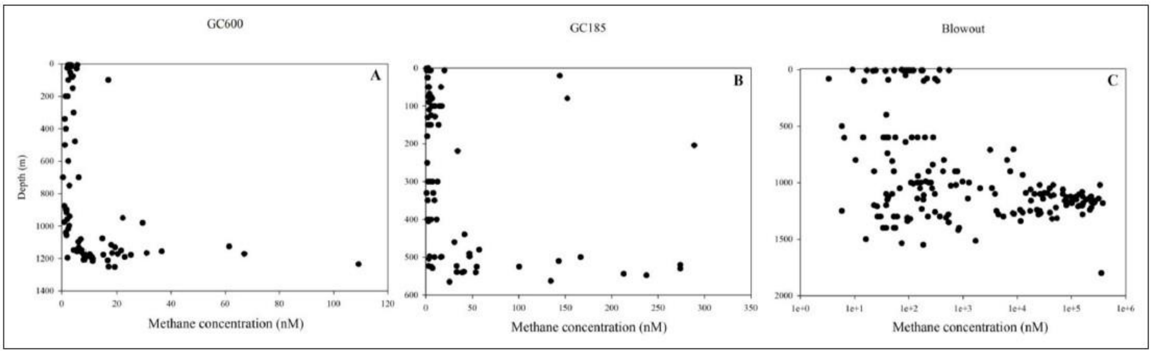

Figure 27: Concentration depth profiles of methane at two natural seep sites (A, B) and the Deepwater Horizon site (C; derived from Rogener et al., 2018).

The atmospheric emission associated with DWH blowout was measured in mid-June 2010 by Yvon-Lewis et al. (2011), which was before the well head was capped. The flux was 0.362 kg day^{-1} which yields 0.030 tonnes for 84 days when we assume steady-state conditions (*Table 6*). This is much smaller than the flux released at the wellhead and indicates that much methane released was attenuated in the water column. This is also indicated by the aqueous methane concentrations and shows parallels with the fate of methane released at deep natural seeps. The observation by Yvon-Lewis et al. using ship-based measurements is confirmed by Ryerson et al. (2011) who performed aircraft-based monitoring. They found that no atmospheric methane enhancements associated with the spill could be detected at the moment of initial containment and a cap was secured over the wellhead. This is attributed to mixing of air masses impacted by methane sources and sinks unrelated to the spill.

The methane chemistry was also studied after the well was shut-in (*Table* 8). Kessler et al. (2011) observed for the period August – October 2010 that the methane concentrations at the spill site were not exceeding ambient levels for the Gulf of Mexico: the average concentration was 1.4 ± 2.0 nM (i.e. background level) with maximum of 20.4 nM. Monitoring data collected after 2010 is presented by Rogener et al. (2018). For non-seep samples, the concentration range lies just below 10 nmol L^{-1} for 2011 and around 1 nmol L^{-1} for 2012-2014, whereas the methane oxidation rate constant was still elevated for 2011 and 2012 compared to 2013-2015 and also 2001. This indicates that the methane concentrations dropped strongly after the well was shut-in while the methanothrophic community remained more active for a longer period.

6 General Discussion

This study summarised scientific literature that presents quantitative assessments of methane released from the seabed at natural seeps or gas and oil wells in the marine environment of the North Sea and Gulf of Mexico. The associated methane emission at the sea-air interface was also addressed in the investigation. Three topics deserve discussion: 1. availability of data, 2. uncertainties in flux estimates and 3. differences and similarities between the North Sea and the Gulf of Mexico with respect to both natural seeps and potential for man-induced leakage. These topics are addressed below.

6.1 Data availability

Sea-based research is expensive and brings challenges that are not faced as strong for land- based research. This especially holds when research is done at large depths as holds for the deep parts of the Gulf of Mexico. This is reflected in the numbers of studies that have been performed at natural seeps or offshore oil and gas wells. *Table 9* presents the numbers of studies that present quantitative data on methane fluxes at individual sites. Here, distinction is made between natural seeps, regular (abandoned or not) oil or gas wells and sites with catastrophic incidents. Further, distinction is made between investigations at the seabed and at the sea/air interface immediately above the site. This is done as they do not necessarily come together. Note that several studies investigated a number of sites, which ranged up to 14 sites (cf. *Table* 3 and *Table 6*). It is obvious that the numbers are low for all situations where natural seeps have been studied more intensively than wells or blowout and other catastrophic sites. It is especially striking that well leakage has not been studied at the Gulf of Mexico. Neither have blowout sites been studied other than the Deepwater Horizon accident despite a substantial number of blowouts that have happened at the Gulf of Mexico. Izon et al. (2007) stated that blowouts usually ceased either man-induced by pumping mud or cement, or naturally by sediment bridging or depletion of shallow, trapped gas. Unfortunately, there is no scientific proof for this in which it is shown that the sites fulfil natural background conditions.

Table 9. Number of studies with quantitative data on methane fluxes associated with natural seeps or human-induced leakage at regular well sites or well sites with catastrophic events.

	Seeps - seabed	Seeps - sea/air	Well leakage - seabed	Well leakage - sea/air	Catastrophic incident - seabed	Catastrophic incident - sea/air
North Sea	11	2	1	1	1	3
Gulf of Mexico	15	4	0	0	1	2

Table 10 presents the numbers of studies in which the methane fluxes for entire areas have been calculated basically from fluxes per site and site densities. It is clear that a limited amount of studies has been performed. The approaches to estimate seep flux were different among the studies. Site densities were deduced from acoustic measurements for the three studies that addressed natural seepage. When it comes to the two North Sea model studies on methane emission to the air (cf. *Table 4*), the geological and the biological origin may intervene as more intensively studied in the Gulf of Mexico.

Table 10. Number of upscaling studies on methane fluxes due to natural seepage or human-induced leakage at wells sites.

	Seeps - seabed	Natural emission - Sea/air	Well leakage - seabed	Well leakage - sea/air
North Sea	2	4#	2	1
Gulf of Mexico	1	1	0	0

2 studies focus on emissions associated with natural seeps and 2 studies focus on diffusive background emissions (cf. *Table 4*).

6.2 Uncertainties in methane fluxes

It is beyond the scope of this study to establish a rigorous uncertainty analysis on methane fluxes at individual spots and the upscaling to the basin and even global scale. However, a few remarks can be made, several studies presented a range for the methane seepage or atmospheric emission (cf. Tables). The range usually lies within a factor of 2-3 for individual seeps or clusters of seeps. Such a range is rather limited but does not address temporal changes which have also been observed. Jerram et al. (2015) suggested hourly changes in seep intensity of up to one order of magnitude. The temporal changes may be bigger when self-sealing and fracturing by overpressurization happens as observed at seeps where gas hydrate gets formed (Solomon et al., 2008). Some averaging will be at hand when longer time scales and more seeps get considered.

Upscaling to basin scale is determined by two features: density of natural seeps or well leakages and size of fluxes at the individual spots. The first is hard to grasp: some estimates for natural seeps have been made as summarised earlier but the uncertainty in density cannot be deduced from the literature. The upscaling on density of well leakage by Bottner et al. (2020) has been critised by Wilpshaar et al. (2021) as was the range in methane fluxes at leaking wells. The approaches that Judd et al. (1997) and Tizzard (2008) took in their upscaling studies on the range in methane fluxes at natural seeps at the UK Continental Shelf was discussed in section 4.3. Based on that discussion, it seems that there is room for improvement.

When it comes to leakage at wells, the major uncertainty in the associated methane fluxes is primarily related to lack of field data. The number of publicly available scientific studies that quantitatively address methane leakage is very small. No reliable estimates can be made on these methane fluxes for the North Sea and the Gulf of Mexico as study areas.

6.3 Differences and similarities between North Sea and Gulf of Mexico

Geological conditions are widely different for the North Sea and the Gulf of Mexico. From a petroleum-geological point of view, the North Sea can be subdivided into three zones: a northern, a central, and a southern part. The northern North Sea contains many Brent-type fields: mainly Jurassic reservoir rocks, a Jurassic source rock, tilted fault blocks, capped by a thick Tertiary cover. The central North Sea contains many stratigraphic traps, but also structural traps. Reservoirs are of various ages: Paleogene, Chalk, Lower Cretaceous, Triassic, Permian, and even Devonian. Unsurprisingly, there are many different seals in the central part of the North Sea. The southern North Sea is basically a gas province, with Carboniferous source rocks, Permian reservoirs, and thick Permian rock salts acting as seal. Shallow, microbial gas is also present in the southern part.

The Gulf of Mexico is, compared to the North Sea, much more homogeneous with respect to petroleum geology. Deepwater GoM fields all produce from Tertiary sands, thank their existence to the presence of salt structures, and are sourced from a handful of Cretaceous and Jurassic source rocks. The over-all geological characteristics are very similar for an area of some 1000 km long and 200 km wide.

When it comes to methane fluxes at natural seeps, individual seeps release up to 20-40 tonnes methane y^{-1} and seep areas up to 1,000 – 10,000 tonnes y^{-1} as quantified in 26 studies. The range seems to be wider for the North Sea when *Figure 13* and *Figure 23* are compared. These figures also indicate that direct emissions at the sea/air interface are 1-2 order of magnitude lower than the flux at the seabed. However, this observation is based on a very limited number of studies.

One might say that the marine conditions of most of the North Sea and the continental shelf of the Gulf of Mexico are largely similar with respect to depth range and favourable conditions for gas bubbles to reach the sea surface. The seawater temperature at small depths will be higher in the Gulf of Mexico than in the North Sea. This implies that the rates of biogeochemical processes including methane oxidation will be faster when other conditions are comparable. Attenuation of methane released from the seabed will be limited before methane reaches the seawater surface and emissions at the sea-air interface will be closer to fluxes at the seabed compared to methane release from the seabed of the continental slope of the Gulf of Mexico.

The attenuation conditions at the continental slope in the Gulf of Mexico are much different especially for the deepest trajectory. Gas hydrates play an important role in the methane chemistry at the continental slope whereas their role has not been indicated for the North Sea. Attenuation of methane released at the continental slope is favourable where it appears to be unlikely that gas bubbles reach the sea surface and dissolution into seawater is a major process (cf. *Figure 23*). It is unclear what happens with methane released from the seabed after it dissolves into along flowing seawater at the geological time scale. The continuous release of methane from the seabed would result into a continuous build-up of methane in deeper seawater. So the concentration would rise if the build-up is not balanced by methane oxidation or outflow of deep seawater from the Gulf of Mexico towards the Atlantic Ocean. The occurrence or not of the latter has not been addressed in this study. For the North Sea, it is recognised that outflow of methane to the Atlantic Ocean occurs (cf. *Table 4*).

About five times more wells are present in the US territory of the Gulf of Mexico compared to the North Sea. The number of blowouts is considerably higher for the first according to literature. Limited data is present for leakage associated with wells (*Table 9*). Two catastrophic events have been studied in detail: the blowout of the Deep Water Horizon (DWH) in the Gulf of Mexico and that at UK22/4b in the North Sea. The release of methane was 146-200 ktonnes at DWH before the well was killed after 84 days months. At UK22/4b, it is continuous at around 15,000 – 41,000 tonnes y^{-1} since 1990 as this well has not been relieved. Additionally, methane fluxes of 1, 4 and 19 tonnes y^{-1} were observed at three, leaking abandoned Norwegian wells. No other direct measurements on well leakage are known for both areas.

7 Conclusions and Summary

Methane is a greenhouse gas and the concentration in the air is steadily increasing. The marine environment is one of the source areas from which both natural and man-induced emissions originate. Part of the natural emissions originate from seeps and vents at the seabed. Man-induced leakage of methane from the seabed also occurs due to gas flow from subsurface methane-bearing layers along or through offshore oil and gas wells as well as incidental blowouts. For both situations, attenuation of methane may occur before it reaches the sea/air interface in gas bubbles or dissolved state. Methane oxidation, dissolution into seawater and immobilisation as gas hydrates are examples of attenuating processes.

Globally, the natural, geological emission of methane from the marine environment to air is estimated as 5-12 Tg y^{-1} (note 1 Tg = 1 megatonne) whereas that for release from the seabed is estimated as 8- 65 Tg y^{-1}. The difference between the two can be explained by the absorption of methane by seawater on its way up from the seabed to the surface. The global methane release associated with the oil and gas industry is estimated as 68-92 Tg y^{-1}. This number refers to both on- and offshore production and transport and is therefore not suitable for detailed comparisons between natural seepage and anthropogenic leakage.

For the two study areas of the North Sea and the Gulf of Mexico, individual seeps release up to 20-40 tonnes of methane y^{-1} and seep areas up to 1,000 – 10,000 tonnes y^{-1} as quantified in 26 studies. Limited data is present for leakage associated with wells. Two catastrophic events have been studied in detail: the blowout of the Deep Water Horizon (DWH) in the Gulf of Mexico and that at UK22/4b in the North Sea. The release of methane was 146-200 ktonnes at DWH before it was capped after 84 days months. At UK22/4b, it is continuous at around 15,000 – 41,000 tonnes y^{-1} since 1990. Additionally, methane fluxes of 1-, 4-, and 19-ton y^{-1} were observed at three leaking, abandoned Norwegian wells. No other direct measurements on well leakage are known for both areas which hinders quantitative assessments at regional scales.

Incidental upscaling calculations have been made for the North Sea and also natural seepage at the northern continental slope of the Gulf of Mexico. The upscaling calculations for leakage from wells in the North Sea have been criticised by TNO in earlier studies. Reference is made to these studies for the scientific arguments. The calculated ranges for natural seepage at the North Sea and the northern continental slope of Gulf of Mexico are 10,000 – 3,400,000 and 400 – 50,000 tonnes y^{-1}, respectively. The value of 3,400,000 tonnes y^{-1} is remarkably high compared to the estimate for global geological emission from the marine environment (see above). This can be attributed to the way the upper value for the seep flux was calculated: it is statistically based on global data of seeps where global outliers influence the statistics.

Attenuation of methane plays an important role both at the seabed and within the water column. The attenuation of methane in the water column is more favourable for the continental slope of the Gulf of Mexico than the continental shelf of the Gulf and most parts of the North Sea. This is due to the large depth with more favourable conditions for gas hydrate formation, methane oxidation and dissolution of gas bubbles into seawater. It is unclear what the subsequent fate is for methane released from the seabed that dissolves in seawater and flows away from the source zone.

8 References

Bange, H.W., Bartell, U.H., Rapsomanikis, S. & Andreae, M.O. (1994). Methane in the Baltic and North Seas and a reassessment of the marine emissions of methane. Global Biogeochemical Cycles (8), 465-480.

Bernard, B.B., Brooks, J.M., Sackett, W.M. (1976). Natural gas seepage in the Gulf of Mexico. Earth and Planetary Science Letters (31), 48-54.

Bižic, Mina; Grossart, Hans-Peter; and Ionescu, Danny (2020). Methane Paradox. eLS. John Wiley & Sons, Ltd. DOI: 10.1002/9780470015902.a0028892

BOEM (2017). Deepwater Gulf of Mexico. Presentation held at 9 nov 2017, by Mike Celata.

Borges, A.V., Champenois, W., Gypens, N., Delille, B., Harlay, J. (2016). Massive marine methane emissions from near-shore shallow coastal areas. Scientific Reports (6), art. no. 27908.

Bouroullec, R. and Weimer, P. (2017). Geometry and kinematics of Neogene allochthonous salt systems in the Mississippi Canyon, Atwater Valley, western Lloyd Ridge, and western DeSoto Canyon protraction areas, northern deep-water Gulf of Mexico. AAPG Bulletin 101: pp. 1003–1034.

Bouroullec, R., Weimer, P., and Serrano, O. (2017). Petroleum geology of the Mississippi Canyon, Atwater Valley, western DeSoto Canyon, and western Lloyd Ridge protraction areas, northern deepwater Gulf of Mexico: Traps, reservoirs, and tectonostratigraphic evolution. AAPG Bulletin 101, 1073–1108.

Borges, A. V., Champenois, W., Gypens, N., Delille, B., Harlay, J., (2016). Massive marine methane emissions from near-shore shallow coastal areas. Scientific Reports 6, Article number: 27908. Doi: 10.1038/srep27908.

Böttner, C., Haeckel, M., Schmidt, M., Berndt, C., Vielstädte, L., Kutsch, J.A., Weiss, T. (2020). Greenhouse gas emissions from marine decommissioned hydrocarbon wells: leakage detection, monitoring and mitigation strategies. Int. J. Greenhouse Gas Control (100), 103119.

Bowen, J.M. (1991). 25 Years of UK North Sea exploration. In : United Kingdom Oil and Gas Fields, 25 Years Commemorative Volume, Abbotts, I.L. (ed.). Geological Society, London, Memoirs, 14, pp. 1-7.

Brekke, T., Lonne, O., Ohm, S.E. (1997). Light hydrocarbon gases in shallow sediments in the northern North Sea. Mar. Geol. (137), 81–108.

Breunese, J.N., Andersen, J.H., Brinkman, S., Jagosiak, P., Karnin, W-D., Karnkowski, P.H., Kombrink, H., Messner, J., Mijnlieff, H., Olsen, S.B., Peryt, T.M., Piske, J., Poprawa, P., Roelofsen, J.W., Stoker, S.J., Smith, N.J.P., Swann, G., Waksmundzka, M.I. & Veldkamp, J.G. (2010). Reserves and production history. In: Doornenbal, J.C. and Stevenson, A.G. (editors): Petroleum Geological Atlas of the Southern Permian Basin Area. EAGE Publications b.v. (Houten): 271-281.

Brown, S. (1991). Stratigraphy of the oil and gas reservoirs: UK continental shelf. In : United Kingdom Oil and Gas Fields, 25 Years Commemorative Volume, Abbotts, I.L. (ed.). Geological Society, London, Memoirs, 14, p 9–18.

Brufatto, C., Cochran, J., Power, L.C.D., El-Zeghaty, S.Z.A.A., Fraboulet, B., Griffin, T., Munk, S., Justus, F., Levine, J., MontGoMery, C., Murphy, D., Pfeiffer, J., Pornpoch, T., Rishmani, L. (2003). From mud to cement - building gas wells. Schlumb. Oil Field Rev. (15), 62-76.

Clayton, C.J. & Dando, P.R. (1996). Comparison of seepage and seal leakage rates. In ‘’Hydrocarbon mitigation and its near-surface expression’’, eds. D. Schumacher & M.A. Abrams. AAPG Memoir no. 66, 169-171.

Damm, E., Mackensen, A., Budeus, G., Faber, E., & Hanfland C. (2005). Pathways of methane in seawater: Plume spreading in an Arctic shelf environment (SW-Spitsbergen). Continental Shelf Research (25), 1453–1472.

Davies, R.J., Almond, S., Ward. R.S., Jackson, R.B., Adams, C., Worrall, F., Herringsshaw, L.G., Gluyas, J.G. & Whiteshead, M.A. (2014). Oil and gas wells and their integrity: Implications for shale and unconventional resource exploitation. Marine Petrol. Geol. (56), 239-254.

De Bruin, G., ten Veen, J., Wilpshaar, M., Versteijlen, N., Geel, K., Verweij, H. & Carpentier, S. (2022). Origin of shallow gas in the Dutch North Sea — Seismic versus geochemical evidence. Interpretation (10), SB63-SB76.

Eriksen et al (2003) Chapter 20 - Oil and gas resources. In: The Millennium Atlas.

Etiope, G. and Schwietzke, S. (2019). Global geological methane emissions: an update of top- down and bottom-up estimates, Elem. Sci. Anth. (7), 47.

Fan, W., McGuire, J.J. & Shearer, P.M. (2020). Abundant Spontaneous and Dynamically Triggered Submarine Landslides in the Gulf of Mexico. Geophys. Res. Letters. (47), e2020GL087213.

Fisher, C., Roberts, H., Cordes, E. & Bernard, B. (2007). Cold Seeps and Associated Communities of the Gulf of Mexico. Oceanography (20), 118-129.

Frank D.J., Sackett W., Hall R., Fredericks, A. (1970). Methane, ethane, and propane concentrations in Gulf of Mexico. American Association of Petroleum Geologists Bulletin (54), 1933-1938.

Fyfe, J.A., Gregersen, U, Jordt, H, Rundberg, Y, Eidvin, T, Evans, D, Stewart, D, Hovland, M, Andresen, P. (2003). Oligocene to holocene. In: Evans, D, Graham, C, Armour, A, Bathurst, P (Eds.), The Millennium Atlas: Petroleum Geology of the Central and Northern North Sea. Geological Society of London, London, pp. 279–287.

Gast, R.E., Dusar, M., Breitkreuz, C., Gaupp, R., Geissler, M., Schneider, J.W., Stemmerik, L., Geluk, M.C., Kiersnowski, H., Glennie, K.W., Kabel, S. and Jones, N.S. (2010). Rotliegend. In Doornenbal, J.C. and Stevenson, A.G. (editors). Petroleum Geological Atlas of the Southern Permian Basin Area. EAGE Publications b.v.

Gerilowski, K., Krings, T., Hartmann, J., Buchwitz, M., Sachs, T., Erzinger, J., Burrows, J.P. & Bovensmann, H. (2015). Atmospheric remote sensing constraints on direct sea-air methane flux from the 22/4b North Sea massive blowout bubble plume. Marine Petrol. Geol. (68), 824-835.

Hill, P.J., and Wood, G.V. (1980) Geology of the Forties Field, U.K. Continental Shelf, North Sea, in Giant Oil and Gas Fields of the Decade:1968–1978, AAPG Memoir 30

Hjelstuen, B.O. (2010). Sources of methane inferred from pore-water δ13C of dissolved inorganic carbon in Pockmark G11, offshore Mid-Norway. Chem. Geol. (275), 127-138.

Hmiel, B, Petrenko, VV, Dyonisius, MN, Buizert, C, Smith, AM, Place, PF, Harth, C, Beaudette, R, Hua, Q, Yang, B, Vimont, I, Michel, SE, Severinghaus, JP, Etheridge, D, Bromley, T, Schmitt, J, Fain, X,Weiss, RF & Dlugokencky, E. (2020). Preindustrial 14CH4 indicates greater anthropogenic fossil CH4 emissions. Nature (578), 409–412.

Hood K.C., Wenger L.M., Gross O.P., Harrison S.C. (2002). Hydrocarbon systems analysis of the northern Gulf of Mexico: Delineation of hydrocarbon migration pathways using seeps and seismic imaging, in Surface exploration case histories: Applications of geochemistry, magnetics, and remote sensing. In: Schumacher D, LeSchack LA (eds) AAPG Studies in Geology no. 48 and SEG Geophysical References Series no. 11, pp 25–40

Hovland, M. & Sommerville, J.H. (1985). Characteristics of two natural gas seepages in the North Sea. Marine and Petroleum Geology (2), 319-326.

Hovland, M., Judd, A.G. (1992). The global production of methane from shallow submarine sources. Continental Shelf Research (12), 1231-1238.

Hovland, M., Judd, A.G. & Burke, R.A. (1993). The global flux of methane from shallow submarine sediments. Chemosphere (26), 559-578.

Hovland, M. (2007). Discovery of prolific natural methane seeps at Gullfaks, northern North Sea. Geo-Mar Lett (27), 197-201.

Hovland, M., Jensen, S. & Fichler, C. (2012). Methane and minor oil macro-seep systems – Their complexity and environmental significance. Marine Geol. (332-334), 63-173.

Hu, L., Yvon-Lewis, S.A., Kessler, J.D., MacDonald, I.R. (2012). Methane fluxes to the atmosphere from deepwater hydrocarbon seeps in the northern Gulf of Mexico. Journal of Geophysical Research: Oceans, (117), art. no. C01009.

Irakulis-Loitxate, I., Gorrono, J., Zavala-Araiza, D. & Guanter, L. (2022). Satellites Detect a Methane Ultra-emission Event from an Offshore Platform in the Gulf of Mexico. Env. Sci. Technol. Lett. (9), 520-525.

Izon, D., Danenberger, E.P. & Mayes, M. (2007). Absence of fatalities in blowouts encouraging in MMS study of OCS incidents 1992-2006. Well Control, July/August 2007, 84-90.

Jerram, K., Weber, T.C., Beaudoin, J. (2015). Split-beam echo sounder observations of natural methane seep variability in the northern Gulf of Mexico. Geochemistry, Geophysics, Geosystems (16), 736-750.

Johansen, C., Macelloni, L., Natter, M., Silva, M., Woosley, M., Woolsey, A., Diercks, A.R., Hill, J., Viso, R., Marty, E., Lobodin, V.V., Shedd, W., Joye, S.B., MacDonald, I.R. (2020). Hydrocarbon migration pathway and methane budget for a Gulf of Mexico natural seep site: Green Canyon 600. Earth and Planetary Science Letters (545), art. no. 116411, .

Judd, A., Davies, G., Wilson, J., Holmes, R., Baron, G. & Bryden, I. (1997). Contributions to atmospheric methane by natural seepages on the UK continental shelf. Marine Geol. (137), 165-189.

Judd, A. (2004). Natural seabed gas seeps as sources of atmospheric methane. Environ. Geol. (46), 988–996.

Judd, A. & Hovland, M. (2007). Pockmarks, shallow gas, and seeps: an initial appraisal. In ‘’Seabed Fluid Flow. The impact on geology, biology and the marine environment’’, eds. A. Judd & M. Hovland. Cambridge Univ. Press, p. 7-44.

Judd, A. (2015). The significance of the 22/4b blow-out site methane emissions in the context of the North Sea. Marine Petrol. Geol. (68), 836-847.

Kaiser, M.J. (2017). Rigless well abandonment remediation in the shallow water U.S. Gulf of Mexico. J. Petrol Sci. Eng. (151), 94–115.

Kennicutt, M.C. (2017) Oil and gas seeps in the Gulf of Mexico. In: C.H. Ward (ed.), Habitats and Biota of the Gulf of Mexico: Before the Deepwater Horizon Oil Spill, DOI 10.1007/978-1- 4939-3447-8_5

Kessler, J.D., Valentine, D.L., Redmond, M.C., Du, M., Chan, E.W., Mendes, S.D., Quiroz, E.W., Villanueva, C.J., Shusta, S.S., Werra, L.M., Yvon-Lewis, S.A. & Weber, T.C. (2011). A persistent oxygen anomaly reveals the fate of spilled methane in the deep Gulf of Mexico. Science (331), 312-315.

Krämer, K., Holler, P., Herbst, G., Bratek, A., Ahmerkamp, S., Neumann, A., Bartholoma, A., Beusekom van, J.E.E., Holtappels, M., Winter, C. (2017). Abrupt emergence of a large pockmark field in the German Bight, southeastern North Sea. Scientific Reports (7), 5150.

Kvenvolden, K.A., Lorenson, T.D., Reeburgh, W.S. (2001). Attention turns to naturally occurring methane seepage. EOS, Transactions, American Geophysical Union (82), 457-458.

Landrø, M., Wehner, D., Vedvik, N., Ringrose, P., Løhre, N.L., Berteussen, K. (2019). Gas flow through shallow sediments—a case study using passive and active seismic field data. Int. J. Greenhouse Gas Control (87), 121–133.

Lapham et al., Lapham, L.L., Alperin, M., Chanton, J., Martens, C. (2008). Upward advection rates and methane fluxes, oxidation, and sources at two Gulf of Mexico brine seeps. Marine Chemistry (112), 65-71.

Leifer, I. (2015). Seabed bubble flux estimation by calibrated video survey for a large blowout seep in the North Sea. Marine Petrol. Geol. (68), 743-752.

Leifer, I. & Judd, A. (2015). The UK22/4b blowout 20 years on: Investigations of continuing methane emissions from sub-seabed to the atmosphere in a North Sea context. Marine Petrol. Geol. (68), 706-717.

Leonte, M., Wang, B., Socolofsky, S.A., Mau, S., Breier, J.A., Kessler, J.D. (2018). Using Carbon Isotope Fractionation to Constrain the Extent of Methane Dissolution Into the Water Column Surrounding a Natural Hydrocarbon Gas Seep in the Northern Gulf of Mexico. Geochemistry, Geophysics, Geosystems, (19), 4459-4475.

Li, J., Roche, B., Bull, J.M., White, P.R., Leighton, T.G., Provenzano, G., Dewar, M., Henstock, T.J. (2020). Broadband Acoustic Inversion for Gas Flux Quantification—Application to a Methane Plume at Scanner Pockmark, Central North Sea. Journal of Geophysical Research: Oceans (125), art. no. e2020JC016360, .

Maloney, J. M., Bentley, S. J., Xu, K., Obelcz, J., Georgiou, I. Y., Jafari, N. H., & Miner, M. D. (2019). Mass wasting on the Mississippi River subaqueous delta. Earth-Science Reviews (200), art. no. 103001.

https://www.marineregions.org. North Sea bathymetry map, retrieved July 30, 2022.

Mau, S., Gentz, T., Korber, J.-H., Torres, M.E., Romer, M., Sahling, H., Wintersteller, P., Martinez, R., Schluter, M. & Helmke, E. (2015). Seasonal methane accumulation and release from a gas emission site in the central North Sea. Biogeosciences (12), 5261-7276.

Meurer, W.P., Blum, J., Shipman, G. (2021). Volumetric Mapping of Methane Concentrations at the Bush Hill Hydrocarbon Seep, Gulf of Mexico. Frontiers in Earth Science (9), art. no. 604930, .

Milkov, A.V. & Sassen, R. (2002). Economic geology of the Gulf of Mexico and the Blake Ridge Gas Hydrate Provinces. Gulf coast association of geological societies transactions (LI), 219- 228.

Missiaen, T., Murphy, S., Loncke, L., Henriet, J.-P. (2002). Very high-resolution seismic mapping of shallow gas in the Belgian coastal zone. Cont. Shelf Res. (22), 2291–2301.

Nehring, R. (1991). Oil and Gas resources. In: The Geology of North America Vol. J, The Gulf of Mexico Basin. The Geological Society of America, 1991, pp. 445-494.

Nilsen, L.H. (2007). Brønnintegritet I Statoil og på norsk sokkel. Published at the NPF 20‘ Kristiansand Conference [Online]. Available. http://www.npf.no/.

Patruno, S., Kombrink, H., Archer, S.G. (2021) Cross-border stratigraphy of the Northern, Central and Southern North Sea: a comparative tectono-stratigraphic megasequence synthesis. From: PATRUNO, S., ARCHER, S. G., CHIARELLA, D., HOWELL, J. A., JACKSON, C. A.-
L. & KOMBRINK, H. (eds) Cross-Border Themes in Petroleum Geology I: The North Sea. Geological Society, London, Special Publications, 494, https://doi.org/10.1144/SP494- 2020-228

Peel, F.J., Travis, C.J. and Hossack, J.R. (1995). Genetic structural provinces and salt tectonics of the Cenozoic offshore U.S. Gulf of Mexico: A preliminary analysis. In Salt Tectonics: A Global Perspective, M.P.A. Jackson, D.G. Roberts, and S. Snelson, eds, American Association of Petroleum Geologists Memoir (65), pp. 153–175.

Pohlman, J.W., Canuel, E.A., Chapman, N.R., Spence, G.D., Whiticar, M.J., Coffin, R.B. (2005). The origin of thermogenic gas hydrates on the northern Cascadia Margin as inferred from isotopic (13C/12C and D/H) and molecular composition of hydrate and vent gas. Organic Geochemistry (36), 703-716.

Pulster E.L., Gracia A., Armenteros M., Toro-Farmer G., Snyder S.M., Carr B.E., Schwaab, M.R., Nicholson, T.J., Mrowicki, J. & Murawski, S.A.. A first comprehensive baseline of hydrocarbon pollution in Gulf of Mexico fishes. Sci Rep 2020; 10:6437. Doi: 10.1038/s41598-020-62944-6

Rakowski, C.V., Magen, C., Bosman, S., Rogers, K.L., Gillies, L.E., Chanton, J.P., Mason, O.U. (2015). Methane and microbial dynamics in the Gulf of Mexico water column. Frontiers in Marine Science (2), art. no. 69.

Randhol, P., Carlsen, I.M. (2007). Presentation Assessment of Sustained Well Integrity on the Norwegian Continental Shelf. SINTEF Petroleum Research

Rehder, G., Keir, R.S. & Pohlmann, T. (1998). The multiple sources and patterns of methane in North Sea Waters. Aq. Geochem. (4), 403-427.

Rogener, M.K., Bracco, A., Hunter, K.S., Saxton, M.A., Joye, S.B. (2018). Long-term impact of the Deepwater Horizon oil well blowout on methane oxidation dynamics in the northern Gulf of Mexico. Elementa (6), art. no. 73.

Romer, M., Wenau, S., Mau, S., Veloso, M., Greinert, J., Schluter, M., Bohrmann, G. (2017). Assessing marine gas emission activity and contribution to the atmospheric methane inventory: a multidisciplinary approach from the Dutch Dogger Bank seep area (North Sea). Geochem., Geophys., Geosyst. (18), 2617–2633.

Romer, M., Hsu, C.-W., Loher, M., MacDonald, I.R., dos Santos Ferreira, C., Pape, T., Mau, S., Bohrmann, G., Sahling, H. (2019). Amount and Fate of Gas and Oil Discharged at 3400 m Water Depth From a Natural Seep Site in the Southern Gulf of Mexico. Frontiers in Marine Science (6), art. no. 700, .

Romer, M., Blumenberg, M., Heeschen, K., Schloemer, S., Müller, H., Müller, S., Hilgenfeldt, C., Barckhausen, U., Schwalenberg, K. (2021). Seafloor methane seepage related to salt diapirism in the Northwestern Part of the German North Sea. Front. Earth Sci. (9), 556329.

Ryerson, T.B., Aikin, K.C., Angevine, W.M., Atlas, E.L., Blake, D.R., Brock, C.A., Fehsenfeld, F.C., Gao, R.-S., De Gouw, J.A., Fahey, D.W., Holloway, J.S., Lack, D.A., Lueb, R.A., Meinardi, S., Middlebrook, A.M., Murphy, D.M., Neuman, J.A., Nowak, J.B., Parrish, D.D., Peischl, J., Perring, A.E., Pollack, I.B., Ravishankara, A.R., Roberts, J.M., Schwarz, J.P., Spackman, J.R., Stark, H., Warneke, C., Watts, L.A. (2011). Atmospheric emissions from the deepwater Horizon spill constrain air-water partitioning, hydrocarbon fate, and leak rate. Geophysical Research Letters (38), art. no. L07803

Sassen, R., Milkov, A.V., Roberts, H.H., Sweet, S.T., DeFreitas, D.A. (2003). Geochemical evidence of rapid hydrocarbon venting from a seafloor-piercing mud diapir, Gulf of Mexico continental shelf. Marine Geology (198), 319-329.

Saunois, M, Stavert, AR, Poulter, B, Bousquet, P, Canadell, JG, Jackson, RB, Raymond, PA, Dlugokencky, EJ, Houweling, S, Patra, PK, Ciais, P, Arora, VK, Bastviken, D, Bergamaschi, P, Blake, DR, Brailsford, G, Bruhwiler, L, Carlson, KM, Carrol, M, Castaldi, S, Chandra, N, Crevoisier, C, Crill, PM, Covey, K, Curry, CL, Etiope, G, Frankenberg, C, Gedney, N, Hegglin, MI, Hoglund- Isaksson, L, Hugelius, G, Ishizawa, M, Ito, A, Janssens-Maenhout, G, Jensen, KM, Joos, F, Kleinen, T, Krummel, PB, Langenfelds, RL, Laruelle, GG, Liu, L, Machida, T, Maksyutov, S, McDonald, KC, McNorton, J, Miller, PA, Melton, JR, Morino, I, Muller, J, Murguia-Flores, F, Naik, V, Niwa, Y, Noce, S, O'Doherty, S, Parker, RJ, Peng, C, Peng, S, Peters, GP, Prigent, C, Prinn, R, Ramonet, M, Regnier, P, Riley, WJ, Rosentreter, JA, Segers, A, Simpson, IJ, Shi, H, Smith, SJ, Steele, LP, Thornton, BF, Tian, H, Tohjima, Y, Tubiello, FN, Tsuruta, A, Viovy, N, Voulgarakis, A, Weber, TS, van Weele, M, van der Werf, GR, Weiss, RF, Worthy, D,Wunch, D, Yin, Y, Yoshida, Y, Zhang,W, Zhang, Z, Zhao, Y, Zheng, B, Zhu, Q, Zhu, Q & Zhuang, Q. 2020. The global methane budget 2000–2017. Earth System Science Data 12: 1561–1623. DOI: https://doi.org/10.5194/essd-12-1561- 2020.

Schneider von Deimling, J., Rehder, G., Greinert, J., McGinnnis, D.F., Boetius, A., Linke, P. (2011). Quantification of seep-related methane gas emissions at Tommeliten, North Sea. Continental Shelf Research (31), 867-878.

Schneider von Deimling, J., Linke, P., Schmidt, M. & Rehder, G. (2015). Ongoing methane discharge at well site 22/4b (North Sea) and discovery of a spiral vortex bubble plume motion. Marine Petrol. Geol. (68), 718-730.

Schroot, B.M., Klaver, G. & Schuttenhelm, R.T.E. (2005). Surface and subsurface expressions of gas seepage to the seabed – examples from the Southern North Sea. Marine Petrol. Geol. (22), 499-515.

Scranton, M.I. & McShane, K. (1991). Methane fluxes in the southern North Sea: the role of European rivers. Cont. Shelf Res. (11), 37-52.

Silva, M., Roa, C., Ali, N.B.H., O'Reilly, C., Abichou, T., MacDonald, I.R. (2022). Fate of Methane Released From a Destroyed Oil Platform in the Gulf of Mexico. Frontiers in Earth Science (10), art. no. 833661.

Solomon, E.A., Kastner, M., Jannasch, H., Robertson, G., Weinstein, Y. (2008). Dynamic fluid flow and chemical fluxes associated with a seafloor gas hydrate deposit on the northern Gulf of Mexico slope. Earth and Planetary Science Letters (270), 95-105.

Solomon, E.A., Kastner, M., MacDonald, I.R., Leifer, I. (2009). Considerable methane fluxes to the atmosphere from hydrocarbon seeps in the Gulf of Mexico. Nature Geoscience (2), 561- 565.

Soto, L.A., Botello, A.V., Licea-Durán, S., Lizárraga-Partida, M.L. & Yáñez-Arancibia, A. (2014). The environmental legacy of the Ixtoc-I oil spill in Campeche Sound, southwestern Gulf of Mexico. Front. Mar. Sci. (1), article no. 57

Suess, E. (2010). 12 Marine cold seeps. In K. N. Timmis (ed.), Handbook of Hydrocarbon and Lipid Microbiology, Springer-Verlag Berlin Heidelberg, p. 188-203.

Tizzard, L. (2008). The Contribution to Atmospheric Methane from Sub-seabed Sources in the UK Continental Shelf. Unpublished PhD-thesis, University of Newcastle upon Tyne, UK.

Thornton, BF, Etiope, G, Schwietzke, S, Milkov, AV, Klusman, RW, Judd, A, & Oehler, DZ. (2021). Conflicting estimates of natural geologic methane emissions. Elem Sci Anth (9), 1.

TNO (2018). Emissie van het broeikasgas methaan gerelateerd aan de olie- en gassector in Nederland met nadruk op exploratie en productie. TNO2018 R11080 https://www.nlog.nl/methaanemissies.

TNO (2019). Inventory of wells through shallow gas layers in the Dutch North Sea. TNO2019 R11562; https://www.nlog.nl/en/papers.

Upstill-Goddard, R.C., Barnes, J., Frost, T., Punshon, S. & Owens, N.J.P. (2000). Methane in the southern North Sea: Low-salinity inputs, estuarine removal, and atmospheric flux. Global Biogeo. Cycles (14), 1205-1217.

Upstill-Goddard, R.C. & Barnes, J. (2016). Methane emissions from UK estuaries: Re-evaluating the estuarine source of tropospheric methane from Europe. Marine Chem. (180), 14-23.

US-EPA (2010). Methane and Nitrous Oxide Emissions From Natural Sources, U.S. Environmental Protection Agency, Office of Atmospheric Programs (6207J), EPA 430-R-10- 001, Washington, DC, 20460,

Valentine, D.L., Blanton, D.C., Reeburgh, W.S. & Kastner, M. (2001). Water column methane oxidation adjacent to an area of active hydrate dissociation, Eel River Basin. Geochim. Cosmochim. Acta (65), 2633-2640.

Van Wijhe, D. H., Lutz, M. & Kaasschieter, J. P. H. (1980). The Rotliegend in the Netherlands and its gas accumulations. Geologie en Mijnbouw (59), 3– 24.

Verweij, J. M., Nelskamp, S. N., ten Veen, J. H., de Bruin, G., Geel, C. R., Donders, T. H. (2018) Generation, migration, entrapment and leakage of microbial gas in the Dutch part of the Southern North Sea Delta. Marine and Petroleum Geology (97), 493–516.

Vielstädte, L., Karstens, J., Haeckel, M., Schmidt, M., Linke, P., Reimann, S., Liebetrau, V., McGinnis, D.F. & Wallmann, K. (2015). Quantification of methane emissions at abandoned gas wells in the Central North Sea. Marine Petrol. Geol. (68), 848-860.

Vielstädte, L., Haeckel, M., Karstens, J., Linke, P., Schmidt, M., Steinle, L. & Wallmann, K. (2017). Shallow gas migration along hydrocarbon wells – An unconsidered, anthropogenic source of biogenic methane in the North Sea. Env. Sci. Technol. (51), 10262-10268.

Vignes, B., (2011). Contribution to well integrity and increased focus on well barriers from a life- cycle aspects. PhD thesis, University of Stavanger, Norway.

Vignes, B., Aadnøy, B.S. (2010). Well-integrity issues offshore Norway. SPE 112535.

Wang, B., Socolofsky, S.A. (2015). A deep-sea, high-speed, stereoscopic imaging system for in situ measurement of natural seep bubble and droplet characteristics. Deep-Sea Research Part I: Oceanographic Research Papers (104), 134-148.

Wang, B., Jun, I., Socolofsky, S.A., DiMarco, S.F., Kessler, J.D. (2020). Dynamics of Gas Bubbles From a Submarine Hydrocarbon Seep Within the Hydrate Stability Zone. Geophysical Research Letters (47), art. no. e2020GL089256.

Wankel, S.D., Joye, S.B., Samarkin, V.A., Shah, S.R., Friederich, G., Melas-Kyriazi, J., Girguis, P.R. (2010). New constraints on methane fluxes and rates of anaerobic methane oxidation in a Gulf of Mexico brine pool via in situ mass spectrometry. Deep-Sea Research Part II: Topical Studies in Oceanography (57), 2022-2029.

Weber, T.C., Jerram, K., Rzhanov, Y., Mayer, L., Lovalvo, D. (2013). Acoustic and optical observations of methane gas seeps in the Gulf of Mexico. Proceedings of Meetings on Acoustics, 19, art. no. 075046, 8 p.

Weber, T.C., Mayer, L., Jerram, K., Beaudoin, J., Rzhanov, Y., Lovalvo, D. (2014). Acoustic estimates of methane gas flux from the seabed in a 6000 km2 region in the Northern Gulf of Mexico. Geochemistry, Geophysics, Geosystems (15), 1911-1925.

Weimer, P., Bouroullec, R., Adson, J., Cossey, S.P.J. (2017). An overview of the petroleum systems of the northern deep-water Gulf of Mexico. AAPG Bulletin (101), 941–993.

Wilpshaar, M., de Bruin, G., Versteijlen, N., van der Valk, K. & Griffioen, J. (2021). Comment on “Greenhouse gas emissions from marine decommissioned hydrocarbon wells: leakage detection, monitoring and mitigation strategies” by Christoph Böttner, Matthias Haeckel, Mark Schmidt, Christian Berndt, Lisa Vielstädte, Jakob A. Kutsch, Jens Karstens & Tim Weiß. Int. J. Greenhouse Gas Control (110), 103395.

Wilson, R.M., Macelloni, L., Simonetti, A., Lapham, L., Lutken, C., Sleeper, K., D'Emidio, M., Pizzi, M., Knapp, J., Chanton, J. (2014). Subsurface methane sources and migration pathways within a gas hydrate mound system, Gulf of Mexico. Geochemistry, Geophysics, Geosystems (15),

89-107.
Yacovitch, T.I., Daube, C., Herndon, S.C. (2020). Methane Emissions from Offshore Oil and Gas Platforms in the Gulf of Mexico. Environmental Science and Technology (54), 3530-3538.
Yvon-Lewis, S.A., Hu, L., Kessler, J. (2011). Methane flux to the atmosphere from the Deepwater Horizon oil disaster. Geophysical Research Letters (38), art. no. L01602.